A relaxation scheme for the simulation of two-phase flows with inaccessible pore volume in polymer flooding

C. Berthon[b,*], B. Braconnier[a], G. L. Dongmo Nguepi[a], C. Preux[a], Q. H. Tran[a]

[a] *IFP Energies nouvelles, 1 et 4 avenue de Bois Préau, 92852 Rueil-Malmaison Cedex, France*

[b] *Université de Nantes, Laboratoire Mathématiques Jean Leray, 2 rue de la Houssinière, BP 92208, 44322 Nantes Cedex 3, France*

Abstract

The simulation of polymer injection in a reservoir is of paramount importance in enhanced oil recovery. Despite decades of research, the computation of polymer flows in porous media remains a challenging task. The main difficulty lies in the necessity to take into account the effect of *inaccessible pore volumes* (IPV), for which standard closure laws give rise to a weakly hyperbolic or even non-hyperbolic system. In the latter case, exponential instabilities may appear at the continuous level, which must be addressed at the discrete level so as to prevent a premature stop of the numerical simulations.

The notion of IPV was introduced by engineers in order to account for the following observation: when a polymer solution is injected into an initial core saturated with water, the breakthrough of the polymer at the exit occurs before that of the water in which it is injected. It seems that due to their large size, the polymer molecules cannot insinuate themselves into all pores as well as water. Having less volume to flood, the polymer molecules see their speed increased, hence the ad hoc acceleration factor associated with the polymer.

In this work, we propose a relaxation method that guarantees some practical robustness for all IPV laws. This is achieved by replacing the original system by a relaxation model which is always hyperbolic. The designed relaxation model involves two parameters which enable us not only to adjust the correct amount of numerical dissipation, but also to ensure positivity for some critical quantities such as water saturation and polymer concentration. Extensive numerical tests are performed in order to compare the relaxation scheme to the more classical upwind scheme for several IPV laws.

Keywords: polymer flooding, inaccessible pore volume, system of conservation laws, weak hyperbolicity, ellipticity, relaxation method, finite-volume scheme, positivity-preserving

*Corresponding author: `christophe.berthon@univ-nantes.fr`

Email addresses: `christophe.berthon@univ-nantes.fr` (C. Berthon), `benjamin.braconnier@ifpen.fr` (B. Braconnier), `guissel_dongmo@yahoo.fr` (G. L. Dongmo Nguepi), `christophe.preux@ifpen.fr` (C. Preux), `quang-huy.tran@ifpen.fr` (Q. H. Tran)

2020 MSC: 35L65, 65M08, 76S05

1. Introduction

1.1. Context and objectives

We are concerned with the numerical approximation of the solutions of a system of conservation laws arising in the modeling of two-phase polymer flows in porous media. Polymer flooding is a *chemical-enhanced oil recovery* (CEOR) process commonly used by reservoir engineers to boost extraction rate. Indeed, injection of a polymer is aimed at increasing the water viscosity and lowering its mobility [29, 21], thus avoiding hydrodynamic instabilities of water-oil fronts [37] and enabling oil to be better produced.

One of the most notorious difficulties in this area is how to correctly take into account the effect of *inaccessible pore volume* (IPV). In CEOR, the polymer is considered to be only transported in the water phase. Due to their bigger size, polymer molecules cannot penetrate all the pores of the medium, unlike smaller water molecules. Having less volume to flood, they can flow faster at an increased or *enhanced* velocity [15, 38]. This acceleration phenomenon is usually introduced into physical models by means of an IPV factor $\gamma \geq 1$ that measures the ratio between the polymer velocity and the water velocity. The algebraic law expressing γ as a function of the water saturation s and the polymer concentration c is mostly empirical and raises two issues:

1. When combined with a flow model consisting of conservation laws [34, 9], for instance, the one-dimensional fractional flow model [34]

$$\partial_t(s) \ + \partial_x(f) \quad = 0, \tag{1.1a}$$
$$\partial_t(sc) + \partial_x(fc\gamma) = 0, \tag{1.1b}$$

   it may yield an ill-posed or locally *elliptic* system: there exist states $\mathbf{w} = (s, sc)$ at which the eigenvalues of the Jacobian matrix $\nabla_{\mathbf{w}}\mathbf{f}(\mathbf{w})$ of the flux $\mathbf{f}(\mathbf{w}) = (f(s,c), f(s,c)c\gamma(s,c))$ are conjugate complex numbers with nonzero imaginary part. Loss of *weak hyperbolicity* (real eigenvalues) at these states is a major obstruction to the stability of linear perturbations [20, 30]. This question pertains to physical modeling and was addressed in [5], further to previous works by Bartelds et al. [2] and Hilden et al. [23].
2. There is an acute need for practitioners to have an efficient simulation tool at their disposal in order to roughly compare different IPV laws to each other, even "inappropriate" ones for which weak hyperbolicity is not guaranteed everywhere for system (1.1) or for a more sophisticated flow model (e.g., with adsorption). This need has necessitated the development of various high order schemes [36, 31, 8, 9] based on upwinding. However, not all of these schemes are capable of coping with the local peaks of polymer concentration that are likely to appear when the IPV law brings

an intrinsic instability to the model. The present contribution is focused on the design of a numerical method that would enable users to freely switch between "good" and "bad" IPV laws with reasonable confidence in the robustness of the code.

By "robustness" we do not mean that the code should avoid crash at all cost. Due to a polynomial or exponential in time accumulation phenomenon stemming from the model, crashes are inevitable since the numbers stored in the computer memory grow larger and larger. Our objective is to ensure that there is enough, but not too much, numerical viscosity introduced by the scheme so that the numerical results are physically relevant. Another goal we want to achieve is to *preserve positivity*, that is, guarantee that the water saturation s remain in the interval $[0, 1]$ and the polymer concentration c remain non-negative. We also require the scheme to provide a satisfactory numerical treatment to the physically important *empty* states for which $s = 0$.

1.2. Methodology and outline

In light of the above objectives, we claim that *relaxation* methods offer a promising approach to be explored. Indeed, the algebraic complexity due to a non-trivial IPV law $\gamma \neq 1$ makes it infeasible to deploy classical approximate Riemann solvers [35, 22] in which the eigen-structure of the exact Jacobian matrix must be known. Even for the Rusanov scheme, an estimate of the largest (supposedly real) eigenvalue is needed, which is not available here. The general theory of relaxation for PDEs expounded by [32, 13] was historically turned by Jin and Xin [27] into a numerical scheme that managed to break free from the nonlinearities of the original system and in which all components of the flux vector are relaxed. Further contributions by Suliciu [39, 40] suggested to relax only the genuine nonlinearities of the system. This idea of partial relaxation has then proved successful in a wide variety of applications (see, e.g., [14, 26, 6, 12, 1]).

To unfold this versatile philosophy, we first propose to cast system (1.1) under a form that is closer to hydrodynamics, namely,

$$\partial_t(s) + \partial_x(su) = 0, \tag{1.2a}$$
$$\partial_t(sc) + \partial_x(scu + q) = 0, \tag{1.2b}$$

where the quantities

$$u(s,c) = \frac{f(s,c)}{s} \qquad \text{and} \qquad q(s,c) = (\gamma(s,c) - 1)\, f(s,c)c \tag{1.3}$$

stand for the two nonlinearities to be relaxed. The reformulated system (1.2) is next approximated by the relaxation model

$$\partial_t(s) + \partial_x(sU) = 0, \tag{1.4a}$$
$$\partial_t(sc) + \partial_x(scU + Q) = 0, \tag{1.4b}$$
$$\partial_t(sU) + \partial_x(sU^2) + (a/s)^2\partial_x(s) = \varepsilon^{-1} s\, (u(s,c) - U), \tag{1.4c}$$

$$\partial_t(sQ) + \partial_x(sQU) + b^2\partial_x(c) \qquad = \varepsilon^{-1} s\ (q(s,c) - Q), \tag{1.4d}$$

for $\varepsilon > 0$ and in which the new variables U and Q stand for the relaxation counterparts of $u(s,c)$ and $q(s,c)$. Finally, to deal with empty states ($s = 0$), we adopt Bouchut's approach [7] which stipulates that the two relaxation parameters a and b are subject to the evolution equations

$$\partial_t(sa) + \partial_x(saU) = 0, \tag{1.5a}$$

$$\partial_t(sb) + \partial_x(sbU) = 0. \tag{1.5b}$$

These parameters are reinitialized at the beginning of each time iteration according to a set of subcharacteristic conditions that rely on the Majda-Pego heuristics [33]. They can be further locally increased in order to enforce positivity of s and c.

To our knowledge, no relaxation has ever been attempted for models of the type (1.1), even for the simplest case $\gamma = 1$ where it degenerates to a Keyfitz-Kranzer system [28, 25]. Although the two-parameter relaxation strategy (1.4)-(1.5) bears some similarities with that of Baudin et al. [4, 3] for a two-phase drift-flux model, its main novelties lie in the preliminary reformulation (1.2) and in the correct treatment of empty states. Besides, a careful inspection reveals that we find ourselves in a less favorable situation: while in Baudin et al.'s model, the pressure-velocity pair of Riemann invariants are exactly preserved by the relaxation procedure, here the velocity does not remain constant across a contact wave by construction.

This paper is organized as follows. We begin with a description of the physical model considered in §2, where its properties are highlighted depending on the IPV law selected. The relaxation model is presented in §3, together with a Chapman-Enskog analysis [41] from which a first set of conditions on (a, b) are derived. Thanks to linear degeneracy of all eigenfields, the Riemann problem of the relaxation model is easy to solve. The numerical scheme is then defined as Godunov's method for the relaxation model. The emphasis laid on positivity leads to a new set of conditions of (a, b). In §4, numerical simulations are carried out in order to demonstrate the performance of the new scheme on a series of IPV laws in an increasing order of difficulty.

2. Physical model

Let us start with the prototype flow model that will be envisaged throughout this paper. The full set of its balance laws and closure laws are supplied in §2.1. Various examples of IPV laws are detailed in §2.2, along with their respective impact on the hyperbolicity of the model.

2.1. System of equations

We consider a simplified model representing the incompressible flow of a water-polymer mixture and oil in a 1-D porous medium. This simplified model,

which can be derived from a more complete 3-D model (cf. [34, 9, 17] for details), reads

$$\partial_t(s) \ + \partial_x(f) \quad = 0, \tag{2.1a}$$
$$\partial_t(sc) + \partial_x(fc\gamma) = 0, \tag{2.1b}$$

where $s(x,t) \in [0,1]$ denotes the water saturation and $c(x,t) \geq 0$ the polymer concentration. In (2.1), polymer molecules are assumed to be in the water phase only and to not adsorb on the rock. The water fractional flux $f(\cdot,\cdot)$ is a $\mathscr{C}^1$-function of $(s,c) \in [0,1] \times \mathbb{R}_+ =: \Omega$, given by

$$f(s,c) = \frac{\Lambda_w(s)/R(c)}{\Lambda_o(1-s) + \Lambda_w(s)/R(c)}, \tag{2.2}$$

in which:

- $\Lambda_w(s)$ and $\Lambda_o(1-s)$ are respectively the water and oil mobilities[1]. Their definitions involve two parameters $0 \leq s_\flat < s_\sharp \leq 1$ characterizing the porous medium: $s_\flat \in [0,1)$ is the irreducible water saturation, while $1 - s_\sharp \in [0,1)$ is the residual oil saturation[2]. To fix ideas, we take the Brooks-Corey law [10] for relative permeabilties, which yields

$$\Lambda_w(s) = \Lambda_w^{\mathrm{m}} \left(\frac{s - s_\flat}{s_\sharp - s_\flat} \right)_+^{m_w}, \qquad \Lambda_o(1-s) = \Lambda_o^{\mathrm{m}} \left(\frac{s_\sharp - s}{s_\sharp - s_\flat} \right)_+^{m_o}, \tag{2.3}$$

  where $r_+ = \max(r,0)$ stands for the positive part of $r \in \mathbb{R}$ and $(\Lambda_w^{\mathrm{m}}, \Lambda_o^{\mathrm{m}}) \in (\mathbb{R}_+^*)^2$ are two positive constants. The use of the positive part function implies

$$\Lambda_w(s) = 0 \ \text{ for } \ s \in [0, s_\flat], \qquad \Lambda_o(1-s) = 0 \ \text{ for } \ s \in [s_\sharp, 1], \tag{2.4}$$

  which extend the definition of the mobilities over $s \in [0,1]$ without any impact on the fractional flux. Note that to ascertain differentiability of $\Lambda_w(\cdot)$ at $s_\flat$ when $s_\flat > 0$ and of $\Lambda_o(\cdot)$ at $s_\sharp$ when $s_\sharp < 1$, we must require

$$m_w > 1, \qquad m_o > 1. \tag{2.5}$$

  From now on, it is taken for granted that

$$0 \leq s_\flat < s_\sharp \leq 1. \tag{2.6}$$

- $R(c)$ is the mobility reduction factor of the water phase. In real applications, it depends on the polymer adsorption, the water salinity, the

[1] The mobility of each phase is defined as the ratio between the relative permeability $\kappa_r(\cdot)$ and the viscosity μ. In other words, $\Lambda_w(s) = \kappa_{r,w}(s)/\mu_w$ and $\Lambda_o(1-s) = \kappa_{r,o}(1-s)/\mu_o$

[2] In the literature, the notations s_{wi} and s_{or} are commonly used in place of $s_\flat$ and $1 - s_\sharp$.

temperature and the water shear thinning. Here, we restrict ourselves to the analytical formula

$$R(c) = 1 + a_1 c + a_2 c^2 + a_4 c^{15/4}, \qquad a_{1,2,4} \geq 0, \tag{2.7}$$

due to Huggins [24] and extended to high concentration (via the power 15/4) by de Gennes [16]. When $R \equiv 1$, the fractional flux f does not depend on c and boils down to the Buckley-Leverett one [11] for $m_w = m_o = 2$.

In the general case, the fractional flux f satisfies

$$f(s,c) = 0 \ \text{ on } [0, s_\flat] \times \mathbb{R}_+, \qquad f(s,c) = 1 \ \text{ on } [s_\sharp, 1] \times \mathbb{R}_+. \tag{2.8}$$

Furthermore, on $(s_\flat, s_\sharp) \times \mathbb{R}_+$,

$$0 < f(s,c) < 1, \qquad f_s(s,c) > 0, \qquad f_c(s,c) < 0, \tag{2.9}$$

where $f_s(s,c)$ is the partial derivative with respect to s at fixed c and $f_c(s,c)$ is the partial derivative with respect to c at fixed s. In other words, f is an S-shaped function of s at fixed c and a non-increasing function of c at fixed s. From now on, it is convenient to introduce the interstitial velocity

$$u(s,c) = \frac{f(s,c)}{s}, \tag{2.10}$$

which is well-defined for $s \downarrow 0$ when $s_\flat > 0$ and even when $s_\flat = 0$ thanks to (2.5).

The velocity enhancement or IPV factor $\gamma(s,c)$ is continuous and piecewise differentiable function of $(s,c) \in \Omega$. Its derivatives $\gamma_s(s,c)$ and $\gamma_c(s,c)$ are authorized to have jumps over the domain Ω. However, the product $fc\gamma$ must be a $\mathscr{C}^1$ function of $(s,c) \in \Omega$. From physical considerations, it is assumed that

$$\gamma(s,c) \geq 1, \qquad \gamma_s(s,c) \leq 0. \tag{2.11}$$

Several examples will be given in §2.2 for the acceleration factor $\gamma(s,c)$.

Once an IPV law $\gamma(s,c)$ is selected, system (2.1) becomes algebraically closed and can be put under the abstract form

$$\partial_t \mathbf{w} + \partial_x \mathbf{f}(\mathbf{w}) = 0, \tag{2.12}$$

where $\mathbf{w} = (s, sc)^T$ is the vector of conservative variables and $\mathbf{f} = (f, fc\gamma)^T$ is the flux vector. We recall that system (2.12) is said to be

- *hyperbolic* at state $\mathbf{w}$ if the matrix $\nabla_{\mathbf{w}} \mathbf{f}(\mathbf{w})$ possesses two real eigenvalues and if it is real diagonalizable;
- *weakly hyperbolic* at state $\mathbf{w}$ if the matrix $\nabla_{\mathbf{w}} \mathbf{f}(\mathbf{w})$ possesses two real eigenvalues; in case of a double eigenvalue, the eigenspace is not required to be of dimension two;

– *elliptic* at state $\mathbf{w}$ if the matrix $\nabla_{\mathbf{w}}\mathbf{f}(\mathbf{w})$ possesses two conjugate complex eigenvalues with nonzero imaginary parts.

Before launching a simulation, it is essential to know in advance whether system (2.12) is hyperbolic, weakly hyperbolic or elliptic in the region of interest in the state space. The answer to this question depends on the IPV law at hand.

2.2. Laws for IPV factor

Let us review four IPV laws for which we have some knowledge about their hyperbolic vs. elliptic behavior. Visited in the order in which they appeared in the literature, the first three of them (§2.2.1-§2.2.3) are classical while the last one (§2.2.4) is less standard.

2.2.1. No-IPV law

If, for all $(s, c) \in \Omega$,

$$\gamma(s, c) = 1, \tag{2.13}$$

there is no acceleration due to IPV. Model (2.1) then coincides with a Keyfitz-Kranzer system [28], which is weakly hyperbolic in the following sense.

Proposition 2.1. *Model* (2.1) *equipped with the no-IPV law* (2.13) *always has two real eigenfields given by*

	s-wave	*c-wave*
eigenvalue	$f_s = u + su_s$	$f/s = u$
linear degeneracy	–	*yes*
Riemann invariant	c	u
strict Riemann invariant	u	c

On the resonance curve $\Gamma = \big\{(s, c) \mid u_s = 0\big\}$ *where the eigenvalues collapse to each other, the basis of eigenvectors is lost.*

For some initial data, the Riemann problem may have several solutions. Isaacson and Temple [25] advocated an additional entropy condition to recover uniqueness.

2.2.2. Constant IPV law

In reservoir engineering, for want of a better law, the most frequently implemented IPV law is the constant

$$\gamma(s, c) = 1 + \eta, \qquad \eta > 0, \tag{2.14}$$

for all $(s, c) \in \Omega$. The price to be paid for this simplicity is the possible emergence of an elliptic region in the domain Ω, where the eigenvalues are complex. It was shown [2, 23] that this occurs on the manifold $\Gamma = \big\{(s, c) \mid \partial_s u = 0\big\}$ (the resonance curve for the no-IPV law) when $\eta > 0$ is small enough. Hyperbolicity and ellipticity for this system were further clarified [5] as follows.

Theorem 2.1. *Over the region*

$$\mathcal{U} = \big\{(s,c) \in \Omega \,|\, s u_s \leq c u_c\big\}, \tag{2.15}$$

model (2.1) *equipped with the constant IPV law* (2.14) *is weakly hyperbolic for all* $\eta > 0$*. Conversely, if a state* $(s,c) \in \Omega$ *is weakly hyperbolic for model* (2.1) *uniformly in the strength* $\eta > 0$*, then it necessarily belongs to region* $\mathcal{U}$*.*

For any other state $(s,c) \in \Omega \setminus \mathcal{U}$*, there are two amplitudes* $\eta_m(\omega) \geq 0$ *and* $\eta_M(\omega) > 0$ *that depend on the ratio* $\omega = -s u_s/u$ *such that the state is*

- *weakly hyperbolic if* $\eta \in [0, \eta_m(\omega)] \cup [\eta_M(\omega), +\infty)$*;*
- *elliptic if* $\eta \in (\eta_m(\omega), \eta_M(\omega))$*.*

For some initial data, due to elliptic states, polymer accumulation can be observed at the saturation front, which gives rise to very high concentrations and numerical instabilities.

2.2.3. Percolation law

In order to recover real characteristic speeds, Bartelds et al. [2] introduced the saturation-dependent percolation law

$$\gamma(s,c) = \begin{cases} \dfrac{s}{s - s_\bullet} & \text{if } \ s_\flat \leq s \leq 1, \\[2ex] \dfrac{s_\flat}{s_\flat - s_\bullet} & \text{if } \ 0 \leq s \leq s_\flat, \end{cases} \tag{2.16}$$

where $s_\bullet \in (0, s_\flat)$ is the inaccessible pore volume saturation, another characteristic parameter of the medium. Bartelds et al.'s suggestion was actually $s/(s - s_\bullet)$ in the first case $s_\flat \leq s \leq 1$. For $(s,c) \in (s_\flat, 1) \times \mathbb{R}_+$, system (2.1) exhibits a weakly hyperbolic behavior similar to the no-IPV case.

Proposition 2.2. *For* $(s,c) \in (s_\flat, 1) \times \mathbb{R}_+$*, model* (2.1) *equipped with the percolation law* (2.16) *always has two real eigenfields given by*

	s-wave	*c-wave*
eigenvalue	$(su)_s + (\gamma - 1) c u_c$	γu
linear degeneracy	–	*yes*
Riemann invariant	γc	γu
strict Riemann invariant	γu	γc

On the resonance curve $\Gamma = \big\{(s,c) \,|\, s u_s + (\gamma - 1)(c u_c - u) = 0\big\}$ *where the eigenvalues collapse to each other, the basis of eigenvectors is lost.*

The close relationship between the percolation law and the no-IPV law goes much deeper. It turns out that they are in fact equivalent, up to a change of variables. The exact meaning of this statement is elaborated on below.

Theorem 2.2. *The change of variables*

$$\mathtt{S} = s/\gamma, \qquad \mathtt{C} = \gamma c, \qquad \mathtt{F}(\mathtt{S},\mathtt{C}) = f(s,c) \tag{2.17}$$

turns the model (2.1)*, considered for* $(s,c) \in (s_\flat, 1] \times \mathbb{R}_+$ *and equipped with the percolation law* (2.16)*, into the Keyfitz-Kranzer no-IPV model*

$$\partial_t(\mathtt{S}) \quad + \partial_x(\mathtt{F}) \quad = 0, \tag{2.18a}$$

$$\partial_t(\mathtt{SC}) + \partial_x(\mathtt{FC}) = 0, \tag{2.18b}$$

considered for $(\mathtt{S},\mathtt{C}) \in (s_\flat - s_\bullet, 1 - s_\bullet] \times \mathbb{R}_+$*, and conversely. The equivalence between the two systems holds for smooth as well as discontinuous solutions.*

2.2.4. Synthetic law

The percolation law is valid for $0 < s_\bullet < s_\flat$ only. For $s_\bullet > s_\flat > 0$, Hilden et al. [23] advocated two IPV laws called *uniform* and *non-uniform* polymer diffusion based on a less stringent notion of "acceptable" shocks instead of weak hyperbolicity. A *synthetic* law was mathematically built [5] upon Hilden et al.'s law to guarantee global weak hyperbolicity for model (2.1). It reads

$$\gamma(s,c) = \begin{cases} 1 + \dfrac{\eta}{R(c) f(s,c)} & \text{if } \ s \in [s_\bullet, 1], \\ 1 + \dfrac{A(c)}{s^2} + \dfrac{B(c)}{s} & \text{if } \ s \in [s_\flat, s_\bullet], \\ 1 + \dfrac{A(c)}{s_\flat^2} + \dfrac{B(c)}{s_\flat} & \text{if } \ s \in [0, s_\flat], \end{cases} \tag{2.19}$$

where $\eta > 0$ is a given constant and

$$A(c) = \frac{\eta}{R(c)} \frac{s_\bullet^2 u_s(s_\bullet, c)}{u^2(s_\bullet, c)}, \qquad B(c) = \frac{\eta}{R(c)} \frac{u(s_\bullet, c) - s_\bullet u_s(s_\bullet, c)}{u^2(s_\bullet, c)}. \tag{2.20}$$

To express the conditions under which weak hyperbolicity holds, let $s_* \in (s_\flat, s_\sharp)$ be the transition saturation at $c = 0$, that is, the unique solution of

$$u_s(s_*, 0) = 0. \tag{2.21}$$

Uniqueness of s_* follows from the assumptions that the function

$$\Upsilon(s) = -\frac{s \Lambda_o(1-s)}{\Lambda_w(s)} \tag{2.22}$$

is increasing on $(s_\flat, s_\sharp)$, while its derivative Υ' is decreasing on the same interval, with

$$\lim_{s \downarrow s_\flat} \Upsilon'(s) = +\infty, \qquad \lim_{s \uparrow s_\sharp} \Upsilon'(s) = 0. \tag{2.23}$$

It is readily verified that assumptions (2.22)-(2.23) are satisfied by the Brooks-Corey law (2.3) with $m_o \geq m_w > 1$.

Proposition 2.3. *Assume that* $m_o \geq m_w > 1$ *and that*

$$s_\bullet < \min\{2s_\flat,\, s_*\}, \qquad \eta < \frac{s_\bullet^2 u_s(s_\bullet, 0)}{\left\{1 + \dfrac{s_\bullet^2 u_s(s_\bullet, 0)}{u(s_\bullet, 0)}\left[\dfrac{1}{s_\flat} - \dfrac{1}{s_\bullet}\right]\right\}^2}. \tag{2.24}$$

Then, model (2.1) *equipped with the synthetic IPV law* (2.19) *is hyperbolic or weakly hyperbolic everywhere in* Ω*, with at most a resonant saturation.*

3. Numerical scheme

The possibly non-hyperbolic nature of model (2.1) makes it difficult to design a reliable and robust numerical scheme [9, 23]. Here, we take up this challenge by working out a new relaxation scheme in the spirit of Suliciu's method [40]. Our motivation is to supply practitioners with a numerical method whose stability is always guaranteed by the very fact that it can be interpreted as the Godunov scheme applied to a hyperbolic approximation of the original model. In this respect, our approach bears strong similarities with Baudin et al.'s work [4] where the hyperbolicity of the original model is not taken for granted.

3.1. Relaxation model

In accordance with the philosophy of relaxation, we first have to identify the real nonlinearities of model (2.1). To this end, it is judicious to separate those associated with convection from those created by the IPV acceleration. This justifies the reformulation of (2.1) into the form

$$\partial_t(s) \;+ \partial_x(su) \qquad = 0, \tag{3.1a}$$
$$\partial_t(sc) + \partial_x(scu + q) = 0, \tag{3.1b}$$

in which we propose to call the (s, c)-dependent quantity

$$q = (\gamma - 1)scu \tag{3.2}$$

the *IPV deviation*.

We are now able to adapt the relaxation technique by introducing two new variables U and Q to relax $u(s, c)$ and $q(s, c)$. More specifically, we consider the relaxation model

$$\partial_t(s) \;+ \partial_x(sU) \qquad = 0, \tag{3.3a}$$
$$\partial_t(sc) \;+ \partial_x(scU + Q) \qquad = 0, \tag{3.3b}$$
$$\partial_t(sU) + \partial_x(sU^2) + (a/s)^2\partial_x(s) = \varepsilon^{-1}s[u(s, c) - U], \tag{3.3c}$$
$$\partial_t(sQ) + \partial_x(sQU) + b^2\partial_x(c) \qquad = \varepsilon^{-1}s[q(s, c) - Q], \tag{3.3d}$$
$$\partial_t(sa) \;+ \partial_x(saU) \qquad = 0, \tag{3.3e}$$
$$\partial_t(sb) \;+ \partial_x(sbU) \qquad = 0, \tag{3.3f}$$

which is aimed at approximating the original model 2.1 at the continous level. In the right-hand side of (3.3), the parameter $\varepsilon > 0$ plays the role of a characteristic time for the relaxation procedure. The smaller ε is, the closer U and Q are to their equilibrium values $u(s,c)$ and $q(s,c)$. In the left-hand side of (3.3), the positive quantities $a, b > 0$ can be assimilated to Lagrangian velocities. As will be seen later, they must be assigned adequate values at the beginning of each time-step. For the moment, let us observe that they depend on (x,t) and are in fact advected by

$$\partial_t a + U\partial_x a = 0, \tag{3.4a}$$
$$\partial_t b + U\partial_x b = 0, \tag{3.4b}$$

as can be shown by a combination of (3.3e)-(3.3f) with (3.3a). This choice of variable (a,b) instead of constant values, as was previously done in [19], is the standard remedy [7] to deal with possible singularities that appear at empty states $s = 0$. Because a and b depend on (x,t), equations (3.3c)-(3.3d) are not in conservation form. However, dividing (3.3c) by a^2, (3.3d) by b^2 and arguing (3.4), we obtain the balance equations

$$\partial_t\left(\frac{sU}{a^2}\right) + \partial_x\left(\frac{sU^2}{a^2} - \frac{1}{s}\right) = \varepsilon^{-1} s\,\frac{u(s,c) - U}{a^2}, \tag{3.5a}$$
$$\partial_t\left(\frac{sQ}{b^2}\right) + \partial_x\left(\frac{sQu}{b^2} + c\right) = \varepsilon^{-1} s\,\frac{q(s,c) - Q}{b^2}. \tag{3.5b}$$

Then it follows that the relaxation model can be put into the abstract conservation form

$$\partial_t \mathbf{W} + \partial_x \mathbf{F}(\mathbf{W}) = \varepsilon^{-1} s\,\mathbf{R}(\mathbf{W}), \tag{3.6a}$$

with

$$\mathbf{W} = \begin{bmatrix} s \\ sc \\ sU/a^2 \\ sQ/b^2 \\ sa \\ sb \end{bmatrix}, \qquad \mathbf{F}(\mathbf{W}) = \begin{bmatrix} sU \\ scU + Q \\ sU^2/a^2 - 1/s \\ sQU/b^2 + c \\ saU \\ sbU \end{bmatrix}, \qquad \mathbf{R}(\mathbf{W}) = \begin{bmatrix} 0 \\ 0 \\ [u(s,c) - U]/a^2 \\ [q(s,c) - Q]/b^2 \\ 0 \\ 0 \end{bmatrix}. \tag{3.6b}$$

Proposition 3.1. *The homogeneous part of the relaxation model* (3.6)*, i.e., system*

$$\partial_t \mathbf{W} + \partial_x \mathbf{F}(\mathbf{W}) = 0, \tag{3.7}$$

is hyperbolic for all states such that $s > 0$. All of its eigenvalues are linearly

degenerate and are given by

eigenvalue	*Riemann invariants*
U *(double)*	$s\,;\ c\,;\ U\,;\ Q$
$U + a/s$	$c\,;\ Q\,;\ U + a/s\,;\ a\,;\ b$
$U - a/s$	$c\,;\ Q\,;\ U - a/s\,;\ a\,;\ b$
$U + b/s$	$s\,;\ U\,;\ Q - bc\,;\ a\,;\ b$
$U - b/s$	$s\,;\ U\,;\ Q + bc\,;\ a\,;\ b$

Proof. The study of the homogeneous model is made more convenient thanks to primitive variables and the quasi-linear form

$$\partial_t \mathbf{V} + \mathbf{K}(\mathbf{V})\partial_x \mathbf{V} = 0, \tag{3.8a}$$

where

$$\mathbf{V} = \begin{bmatrix} s \\ c \\ U \\ Q \\ a \\ b \end{bmatrix}, \qquad \mathbf{K}(\mathbf{V}) = \begin{bmatrix} U & 0 & s & 0 & 0 & 0 \\ 0 & U & 0 & 1/s & 0 & 0 \\ a^2/s^2 & 0 & U & 0 & 0 & 0 \\ 0 & b^2/s & 0 & U & 0 & 0 \\ 0 & 0 & 0 & 0 & U & 0 \\ 0 & 0 & 0 & 0 & 0 & U \end{bmatrix}. \tag{3.8b}$$

It can be checked that the characteristic polynomial of $\mathbf{K}(\mathbf{V})$ is equal to

$$\mathcal{P}_{\mathbf{K}}(z) = (z-U)^2[(z-U)^2 - a^2/s^2][(z-U)^2 - b^2/s^2], \tag{3.9}$$

from which we infer that all eigenvalues are equal to U (double), $U \pm a/s$ and $U \pm b/s$. Computing the eigenvectors, we find that these eigenfields are all linearly degenerate. The eigenvectors also supply us with the claimed Riemann invariants. We leave this part to the readers. □

3.2. Chapman-Enskog analysis

At the first-order in ε, the structure of the error between the original model (2.1) and the relaxation model (3.3) can be reflected by means of a Chapman-Enskog expansion.

Theorem 3.1. *Let* $\mathbf{W}$ *be the solution of the relaxation model* (3.6) *for a given* $\varepsilon > 0$ *and let* $\mathbf{w} = (s, sc)$ *be the first two components of* $\mathbf{W}$*. Then, in the limit* $\varepsilon \downarrow 0$*, the extracted vector* $\mathbf{w}$ *solves the equivalent equation*

$$\partial_t \mathbf{w} + \partial_x \mathbf{f}(\mathbf{w}) = \varepsilon \partial_x \big\{ [\mathbf{P}(\mathbf{w})]^{-1} [s\mathbf{D}_{a,b}(\mathbf{w})] \mathbf{P}(\mathbf{w})\, \partial_x \mathbf{w} \big\}. \tag{3.10a}$$

with

$$\mathbf{P}(\mathbf{w}) = \begin{bmatrix} 1 & 0 \\ -cs & s \end{bmatrix}, \quad s\mathbf{D}_{a,b}(\mathbf{w}) = \begin{bmatrix} (a/s)^2 - (su_s)^2 - u_c q_s & -u_c(u_s + q_c/s^2) \\ -q_s(s^2 u_s + q_c) & (b/s)^2 - q_s u_c - (q_c/s)^2 \end{bmatrix}. \tag{3.10b}$$

Proof. Assume that the relaxation variables U and Q admit a Chapman-Enskog expansion of the form

$$U = u(s,c) + \varepsilon U^1, \qquad Q = q(s,c) + \varepsilon Q^1. \tag{3.11}$$

Inserting these two expansions into the right-hand sides of equations (3.3c)-(3.3d), we obtain

$$\partial_t(su) + \partial_x(su^2) + (a^2/s^2)\,\partial_x(s) = -sU^1, \tag{3.12a}$$
$$\partial_t(sq) + \partial_x(suq) + \quad b^2\,\partial_x(c) = -sQ^1. \tag{3.12b}$$

To perform the analysis, we need to formulate the first order terms U^1 and Q^1 using only space derivatives. To get rid of time derivatives in equation (3.12), we take advantage of the equations

$$\partial_t s + u\partial_x s + \quad su_s\partial_x s + \quad su_c\partial_x c = 0, \tag{3.13a}$$
$$\partial_t c + u\partial_x c + (q_s/s)\partial_x s + (q_c/s)\partial_x c = 0, \tag{3.13b}$$

which come from the reformulation (3.8) in primitive variables. For instance, adding (3.13a) multiplied by u_s and (3.13b) multiplied by u_c, we get a PDE governing su. Likewise, adding (3.13a) multiplied by q_s and (3.13b) multiplied by q_c, we get a PDE governing sq. After simplification, we end up with

$$\partial_t(su) + \partial_x(su^2) + \quad (s^2u_s^2 + u_cq_s)\,\partial_x s + (s^2u_su_c + u_cq_c)\,\partial_x c = 0, \tag{3.14a}$$
$$\partial_t(sq) + \partial_x(suq) + (s^2q_su_s + q_cq_s)\,\partial_x s + \quad (s^2q_su_c + q_c^2)\,\partial_x c = 0, \tag{3.14b}$$

Combining (3.11) and (3.12), we get an expression for U^1 and Q^1 involving only space derivatives, namely,

$$-sU^1 = (a^2/s^2 - s^2u_s^2 - u_cq_s)\partial_x s + (-s^2u_su_c - u_cq_c)\partial_x c, \tag{3.15a}$$
$$-sQ^1 = \quad (-s^2q_su_s - q_cq_s)\partial_x s + (b^2 - s^2q_su_c - q_c^2)\partial_x c. \tag{3.15b}$$

In matrix-vector language, this can be reformulated as follows:

$$\begin{bmatrix} -U^1 \\ -Q^1 \end{bmatrix} = \mathbf{E}_{a,b}(\mathbf{w})\,\partial_x \begin{bmatrix} s \\ c \end{bmatrix}, \tag{3.16}$$

with

$$\mathbf{E}_{a,b}(\mathbf{w}) = \frac{1}{s}\begin{bmatrix} (a/s)^2 - (su_s)^2 - u_cq_s & -u_c(s^2u_s + q_c) \\ -q_s(s^2u_s + q_c) & b^2 - s^2q_su_c - q_c^2 \end{bmatrix}. \tag{3.17}$$

The values U^1 and Q^1 have been determined with $\partial_x s$ and $\partial_x c$. Now, we have to express them as a function of $\partial_x \mathbf{w}$. To do so, we use the relation

$$\partial_x \begin{bmatrix} s \\ c \end{bmatrix} = \begin{bmatrix} 1 & 0 \\ -c/s & 1/s \end{bmatrix} \partial_x \begin{bmatrix} s \\ sc \end{bmatrix} \tag{3.18}$$

to obtain

$$\begin{bmatrix} -U^1 \\ -Q^1 \end{bmatrix} = \mathbf{E}_{a,b}(\mathbf{w}) \begin{bmatrix} 1 & 0 \\ -c/s & 1/s \end{bmatrix} \partial_x \begin{bmatrix} s \\ sc \end{bmatrix}. \tag{3.19}$$

Equation (3.19) relates U^1 and Q^1 to $\partial_x(s)$ and $\partial_x(sc)$. From the expansion (3.11) and the first two equations (3.3a)-(3.3b), we deduce that

$$\partial_t(s) \ + \partial_x(su) \qquad = \varepsilon \partial_x(s(-U^1)), \tag{3.20a}$$

$$\partial_t(sc) + \partial_x(scu + q) = \varepsilon \partial_x(sc(-U^1) + (-Q^1)), \tag{3.20b}$$

which can be rewritten under the matrix form

$$\partial_t \mathbf{w} + \partial_x \mathbf{f}(\mathbf{w}) = \varepsilon \partial_x \left\{ \begin{bmatrix} s & 0 \\ sc & 1 \end{bmatrix} \mathbf{E}_{a,b}(\mathbf{w}) \begin{bmatrix} 1 & 0 \\ -c/s & 1/s \end{bmatrix} \partial_x \begin{bmatrix} s \\ sc \end{bmatrix} \right\} \tag{3.21}$$

For conciseness, introduce

$$\mathbf{P}(\mathbf{w}) = \begin{bmatrix} 1 & 0 \\ -cs & s \end{bmatrix} \tag{3.22}$$

which is an invertible matrix. Its inverse is given by

$$[\mathbf{P}(\mathbf{w})]^{-1} = \begin{bmatrix} 1 & 0 \\ c & 1/s \end{bmatrix}. \tag{3.23}$$

Then, equation (3.22) can be rewriten as

$$\begin{aligned} \partial_t \mathbf{w} + \partial_x \mathbf{f}(\mathbf{w}) &= \varepsilon \partial_x \left\{ s[\mathbf{P}(\mathbf{w})]^{-1} \mathbf{E}_{a,b}(\mathbf{w}) \begin{bmatrix} 1 & 0 \\ -c/s & 1/s \end{bmatrix} \partial_x \begin{bmatrix} s \\ sc \end{bmatrix} \right\} \\ &= \varepsilon \partial_x \left\{ [\mathbf{P}(\mathbf{w})]^{-1} [s\mathbf{E}_{a,b}(\mathbf{w})] \begin{bmatrix} 1 & 0 \\ -c/s & 1/s \end{bmatrix} [\mathbf{P}(\mathbf{w})]^{-1} \mathbf{P}(\mathbf{w}) \, \partial_x \mathbf{w} \right\}. \end{aligned} \tag{3.24}$$

Defining the matrix

$$\begin{aligned} s\mathbf{D}_{a,b}(\mathbf{w}) &= s\mathbf{E}(\mathbf{w}) \begin{bmatrix} 1 & 0 \\ -c/s & 1/s \end{bmatrix} [\mathbf{P}(\mathbf{w})]^{-1} \\ &= s\mathbf{E}_{a,b}(\mathbf{w}) \begin{bmatrix} 1 & 0 \\ 0 & 1/s^2 \end{bmatrix} \mathbf{P}(\mathbf{w}) [\mathbf{P}(\mathbf{w})]^{-1} = s\mathbf{E}_{a,b}(\mathbf{w}) \begin{bmatrix} 1 & 0 \\ 0 & 1/s^2 \end{bmatrix}, \end{aligned} \tag{3.25}$$

we obtain the equivalent equation (3.10) after some algebra. □

In definition (3.10b) of matrix $s\mathbf{D}_{a,b}(\mathbf{w})$, it is essential to note that the quantities a/s and b/s have been highlighted. In doing so, our goal is to work directly with a/s and b/s (instead of a and b) and to impose conditions on them (§3.3), so that $s\mathbf{D}_{a,b}(\mathbf{w})$ be a "good" matrix even when $s \downarrow 0$. In preparation for this, let us verify that all other terms in $s\mathbf{D}_{a,b}(\mathbf{w})$ also remain well defined.

Lemma 3.1. *If*

$$s_\flat > 0 \qquad or \qquad \Big\{ s_\flat = 0 \ \ and \ \ m_w \geq \tfrac{3}{2} \Big\},$$

then each of the quantities

$$s u_s, \ \ u_c q_s, \ \ s^2 u_s q_s, \ \ q_s q_c, \ \ u_c u_s, \ \ q_s u_c, \ \ (q_c/s)^2, \ \ u_c q_c / s^2$$

has a finite limit when $s \downarrow 0$.

Proof. If $s_\flat > 0$, then u and q vanish identically in a neighborhood of $s = 0$ for all c. Hence, the above quantities also vanish. The last two of them are equal to zero by continuity when $s \downarrow 0$. If $s_\flat = 0$, then up to a c-dependent multiplicative constant we have

$$u \sim s^{m_w - 1}, \qquad q \sim s^{m_w},$$

for $s \downarrow 0$. Then, it is readily checked that

$$\begin{aligned} &s u_s \sim s^{m_w - 1}, \qquad && u_c q_s \sim s^{2m_w - 2}, \qquad && s^2 u_s q_s \sim s^{2m_w - 1}, \qquad && q_s q_c \sim s^{2m_w - 1}, \\ &u_c u_s \sim s^{2m_w - 3}, \qquad && q_s u_c \sim s^{2m_w - 2}, \qquad && q_c / s \sim s^{m_w - 1}, \qquad && u_c q_c / s^2 \sim s^{2m_w - 3}. \end{aligned}$$

Obviously, all of the above quantities have a finite limit if $m_w \geq 3/2$. □

3.3. Conditions on (a, b) for a dissipative limit

The equivalent equation (3.10) is deemed to represent a "good" approximation if the original model (2.1) is a dissipative limit of the relaxation model. Following Majda and Pego's heuristic [33], we require that $[\mathbf{P}(\mathbf{w})]^{-1}][s\mathbf{D}_{a,b}(\mathbf{w})]\mathbf{P}(\mathbf{w})$ be a diffusion matrix. Since this matrix is equivalent to $s\mathbf{D}_{a,b}(\mathbf{w})$, this is equivalent to impose that the eigenvalues of $s\mathbf{D}_{a,b}(\mathbf{w})$ be non-negative. This requirement plays the role of a *Whitham condition* [41] in our problem. The actual derivation of a/s and b/s is inspired from that of Baudin et al. [3, 4] for another problem.

Theorem 3.2. *Let*

$$\mathtt{A}_* = (\sqrt{2} + 1)\sqrt{\Theta} + \mathfrak{G}, \qquad \mathtt{B}_* = (\sqrt{2} - 1)\sqrt{\Theta} + \mathfrak{G}, \tag{3.26}$$

where

$$\Theta = |u_c q_s [u_s + (q_c/s)^2][s^2 u_s + q_c]|, \tag{3.27a}$$

$$\mathfrak{G} = \max\big\{0, \, |u_c q_s| - s^2 u_s^2, \, |q_s u_c| - (q_c/s)^2\big\}. \tag{3.27b}$$

Then, for all a/s and b/s such that

$$\frac{a}{s} > \sqrt{\mathtt{A}_* + (s u_s)^2 + u_c q_s}, \qquad \frac{b}{s} = \sqrt{\mathtt{B}_* + q_s u_c + (q_c/s)^2}, \tag{3.28}$$

the eigenvalues of $s\mathbf{D}_{a,b}(\mathbf{w})$ are real and non-negative.

Proof. Let us assign shorter names to the entries of matrix $s\mathbf{D}_{a,b}(\mathbf{w})$ by writing

$$s\mathbf{D}_{a,b}(\mathbf{w}) = \begin{bmatrix} \mathtt{A} & J \\ K & \mathtt{B} \end{bmatrix}. \tag{3.29a}$$

with

$$\mathtt{A} = (a/s)^2 - (su_s)^2 - u_c q_s, \qquad J = -u_c[u_s + (q_c/s)^2], \tag{3.29b}$$

$$K = -q_s[s^2 u_s + q_c], \qquad \mathtt{B} = (b/s)^2 - q_s u_c - (q_c/s)^2. \tag{3.29c}$$

The characteristic polynomial of $s\mathbf{D}_{a,b}(\mathbf{w})$ is

$$\mathcal{P}(z) = z^2 - (\mathtt{A}+\mathtt{B})z + \mathtt{AB} - JK. \tag{3.30}$$

Its discriminant is equal to

$$\Delta = (\mathtt{A}+\mathtt{B})^2 - 4(\mathtt{AB} - JK) = (\mathtt{A}-\mathtt{B})^2 + 4JK. \tag{3.31}$$

A set of sufficient conditions for the eingenvalues of $s\mathbf{D}(\mathbf{w})$ to be real and non-negative is

$$(\mathtt{A}-\mathtt{B})^2 - 4\Theta \geq 0, \tag{3.32a}$$

$$\mathtt{AB} - \Theta \geq 0, \tag{3.32b}$$

$$\mathtt{A}+\mathtt{B} \geq 0, \tag{3.32c}$$

with

$$\Theta = |JK|. \tag{3.32d}$$

Indeed, condition (3.32a) implies $\Delta \geq 0$. Conditions (3.32b) and (3.32c) respectively imply that the product and the sum of the roots of $\mathcal{P}$ are greater or equal to zero.

System (3.32) is solved by the following three-step procedure:

1. *Solve* $\mathtt{A}+\mathtt{B} \geq 0$. In the $(\mathtt{A},\mathtt{B})$-plane, the set of points satisfying $\mathtt{A}+\mathtt{B}=0$ is the second bisector (in brown in Figure 1). Those points for which $\mathtt{A}+\mathtt{B} \geq 0$ lie above this straight line.
2. *Solve* $\mathtt{AB}-\Theta \geq 0$. The set of points that satisfy $\mathtt{AB}-\Theta=0$ is a hyperbola (in red in Figure 1) which has the axes of coordinates as asymptotes. Those points for which $\mathtt{AB}-\Theta \geq 0$ correspond to the "interior" of the hyperbola.
3. *Solve* $(\mathtt{A}-\mathtt{B})^2 - 4\Theta \geq 0$. The set of points that satisfy $(\mathtt{A}-\mathtt{B})^2 - 4\Theta = 0$ is the pair of lines $\mathtt{B} = \mathtt{A} \pm 2\sqrt{\Theta}$ (in blue in Figure 1). These two lines are parallel to the first bisector. Their ordinates at $\mathtt{A}=0$ are $\mathtt{B} = \pm 2\sqrt{\Theta}$. Those points for which $(\mathtt{A}-\mathtt{B})^2 - 4\Theta \geq 0$ lie outside the strip bordered by these two lines.

The pair of parallel lines $\mathtt{B} = \mathtt{A} \pm 2\sqrt{\Theta}$ intersect the upper arc of hyperbola $\mathtt{AB} = \Theta$ at

$$H_- = \Big((\sqrt{2}+1)\sqrt{\Theta},\, (\sqrt{2}-1)\sqrt{\Theta}\Big), \qquad H_+ = \Big((\sqrt{2}-1)\sqrt{\Theta},\, (\sqrt{2}+1)\sqrt{\Theta}\Big).$$

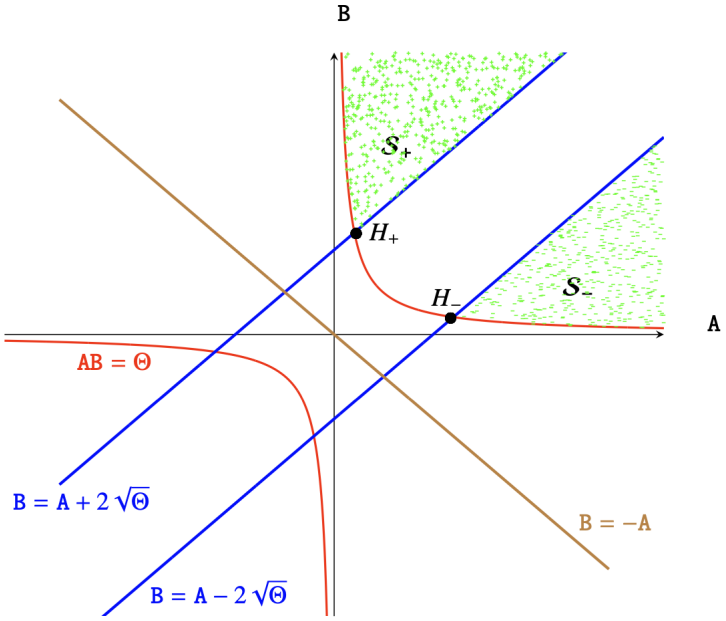

Figure 1: Geometric interpretation of the sufficient conditions (3.32).

We introduce the regions (in green in Figure 1)

$$\mathcal{S}_- = \big\{(\mathtt{A},\mathtt{B}) \;\big|\; \mathtt{A} \geq (\sqrt{2}+1)\sqrt{\Theta},\;\; \mathtt{B} \leq \mathtt{A} - 2\sqrt{\Theta},\;\; \mathtt{AB} - \Theta \geq 0\big\}, \tag{3.33a}$$

$$\mathcal{S}_+ = \big\{(\mathtt{A},\mathtt{B}) \;\big|\; \mathtt{B} \geq (\sqrt{2}+1)\sqrt{\Theta},\;\; \mathtt{B} \geq \mathtt{A} + 2\sqrt{\Theta},\;\; \mathtt{AB} - \Theta \geq 0\big\}. \tag{3.33b}$$

Then, the set of those points $(\mathtt{A},\mathtt{B})$ that satisfy (3.32) coincides with the union $\mathcal{S}_- \cup \mathcal{S}_+$.

Unfortunately, not just any point $(\mathtt{A},\mathtt{B}) \in \mathcal{S}_- \cup \mathcal{S}_+$ is eligible. It is still necessary to be able to invert the relations (3.29b)-(3.29c) to find a/s and b/s from $\mathtt{A}$ and $\mathtt{B}$. Since this inversion is

$$\frac{a}{s} = \sqrt{\mathtt{A} + (su_s)^2 + u_c q_s}, \qquad \frac{b}{s} = \sqrt{\mathtt{B} + q_s u_c + (q_c/s)^2}, \tag{3.34}$$

the quantities under the square root sign must be non-negative. Thus, $\mathtt{A}$ and $\mathtt{B}$ must be large enough. For instance, we can start from H_- and move along the lower blue line until reaching

$$\mathtt{A}_* = (\sqrt{2}+1)\sqrt{\Theta} + \mathfrak{G}, \qquad \mathtt{B}_* = (\sqrt{2}-1)\sqrt{\Theta} + \mathfrak{G}, \tag{3.35a}$$

with

$$\mathfrak{G} = \max\big\{0,\; |u_c q_s| - (su_s)^2,\; |q_s u_c| - (q_c/s)^2\big\}. \tag{3.35b}$$

In this way, we ascertain that $\mathtt{A}_* + (su_s)^2 + u_c q_s \geq 0$ and $\mathtt{B}_* + q_s u_c + (q_c/s)^2 \geq 0$. From this point $(\mathtt{A}_*, \mathtt{B}_*)$, we can now travel rightward along a horizontal line

without leaving $\mathcal{S}_-$. This amounts to increasing a/s while keeping b/s at the same value, which proves (3.28). □

The decision to choose H_- instead of H_+ is also motivated by another reason. By deliberately restricting ourselves to relaxations coefficients such that

$$a/s > b/s > 0, \tag{3.36}$$

we seek a natural ordering of the eigenvalues of the relaxation model, i.e.,

$$U - a/s < U - b/s < U < U + b/s < U + a/s. \tag{3.37}$$

At the discrete level, conditions (3.28) are to be prescribed in each cell and at each time iteration.

By virtue of Lemma 3.1, formulas (3.28) still make sense for $s \downarrow 0$ and even for $s = 0$. From now on, we shall be using the notations

$$\alpha = \frac{a}{s}, \qquad \beta = \frac{b}{s}, \tag{3.38}$$

for convenience. In practice, as will be explained in §3.5, it may be necessary to increase β to enforce positivity of the concentration c. In such a case, we also need to modify α so that the corresponding point $(\mathtt{A}, \mathtt{B})$ remains in $\mathcal{S}_-$.

Lemma 3.2. *Let (α, β) be the pair of relaxation coefficients given by* (3.28)*. For any $\beta' > \beta$, the pair (α', β') is a suitable pair for a dissipative limit provided that*

$$\alpha' > \sqrt{\alpha^2 + (\beta')^2 - \beta^2}. \tag{3.39}$$

Proof. Let $(\mathtt{A}', \mathtt{B}')$ be the point in the plane that corresponds to (α', β'). From

$$\beta' = \sqrt{\mathtt{B}' + q_s u_c + (q_c/s)^2}, \qquad \beta = \sqrt{\mathtt{B}_* + q_s u_c + (q_c/s)^2},$$

we infer that

$$(\beta')^2 - \beta^2 = \mathtt{B}' - \mathtt{B}_*. \tag{3.40}$$

The point $(\mathtt{A}', \mathtt{B}')$ lies in $\mathcal{S}_-$ if

$$\mathtt{A}' > \mathtt{B}' + 2\sqrt{\Theta} = \mathtt{B} + 2\sqrt{\Theta} + (\beta')^2 - \beta^2 = \mathtt{A}_* + (\beta')^2 - \beta^2 \tag{3.41}$$

(we are sure to be above the arc of hyperbola at the bottom of $\mathcal{S}_-$ and do not have to worry about this). The above condition is equivalent to

$$\mathtt{A}' + (su_s)^2 + u_c q_s > \mathtt{A}_* + (su_s)^2 + u_c q_s + (\beta')^2 - \beta^2. \tag{3.42}$$

Since $\alpha^2 > \mathtt{A}_* + (su_s)^2 + u_c q_s$, this can be achieved by imposing the sufficient condition

$$\mathtt{A}' + (su_s)^2 + u_c q_s > \alpha^2 + (\beta')^2 - \beta^2. \tag{3.43}$$

Taking the square root of both sides, we end up with (3.39). □

3.4. Riemann problem

Roughly speaking (cf. §3.6), the relaxation scheme amounts to applying the Godunov scheme to the homogeneous part of the relaxation model. To this end, we have to solve the Riemann problem associated with (3.3), which is easy thanks to linear degeneracy. Let us work with primary variables and consider the initial data

$$\mathbf{V}(x,t=0)=\begin{cases}\mathbf{V}_L & \text{if } x\le 0,\\ \mathbf{V}_R & \text{if } x>0.\end{cases} \tag{3.44a}$$

where

$$\mathbf{V}_L=\begin{bmatrix}s_L\\ c_L\\ U_L\\ Q_L\\ a_L\\ b_L\end{bmatrix},\qquad \mathbf{V}_R=\begin{bmatrix}s_R\\ c_R\\ U_R\\ Q_R\\ a_R\\ b_R\end{bmatrix}. \tag{3.44b}$$

Theorem 3.3. *Assume that $a_L > b_L$ and $a_R > b_R$. The solution of the Riemann problem associated with the relaxation model* (3.3) *and the data* (3.44) *is given by (cf. Figure 2)*

$$\mathbf{V}(x,t)=\begin{cases}\mathbf{V}_L & \text{if } x/t<U^*-a_L/s^*,\\ \mathbf{V}_L^* & \text{if } U^*-a_L/s^*<x/t<U^*-b_L/s^*,\\ \mathbf{V}_L^{**} & \text{if } U^*-b_L/s^*<x/t<U^*,\\ \mathbf{V}_R^{**} & \text{if } U^*<x/t<U^*+b_R/s^*,\\ \mathbf{V}_R^* & \text{if } U^*+b_R/s^*<x/t<U^*+a_R/s^*,\\ \mathbf{V}_R & \text{if } U^*+a_R/s^*<x/t,\end{cases} \tag{3.45a}$$

where

$$\mathbf{V}_L^*=\begin{bmatrix}s^*\\ c_L\\ U^*\\ Q_L\\ a_L\\ b_L\end{bmatrix},\quad \mathbf{V}_L^{**}=\begin{bmatrix}s^*\\ c^*\\ U^*\\ Q^*\\ a_L\\ b_L\end{bmatrix},\quad \mathbf{V}_R^{**}=\begin{bmatrix}s^*\\ c^*\\ U^*\\ Q^*\\ a_R\\ b_R\end{bmatrix},\quad \mathbf{V}_R^*=\begin{bmatrix}s^*\\ c_R\\ U^*\\ Q_R\\ a_R\\ b_R\end{bmatrix}, \tag{3.45b}$$

with

$$\frac{1}{s^*}=\frac{\alpha_L+\alpha_R+(U_R-U_L)}{\alpha_L s_L+\alpha_R s_R}, \tag{3.46a}$$

$$c^*=\frac{\beta_L s_L c_L+\beta_R s_R c_R-(Q_R-Q_L)}{\beta_L s_L+\beta_R s_R}, \tag{3.46b}$$

$$U^*=\frac{\alpha_R s_R U_L+\alpha_L s_L U_R-\alpha_L\alpha_R(s_R-s_L)}{\alpha_L s_L+\alpha_R s_R}, \tag{3.46c}$$

$$Q^*=\frac{\beta_R s_R Q_L+\beta_L s_L Q_R-\beta_L s_L\beta_R s_R(c_R-c_L)}{\beta_L s_L+\beta_R s_R}, \tag{3.46d}$$

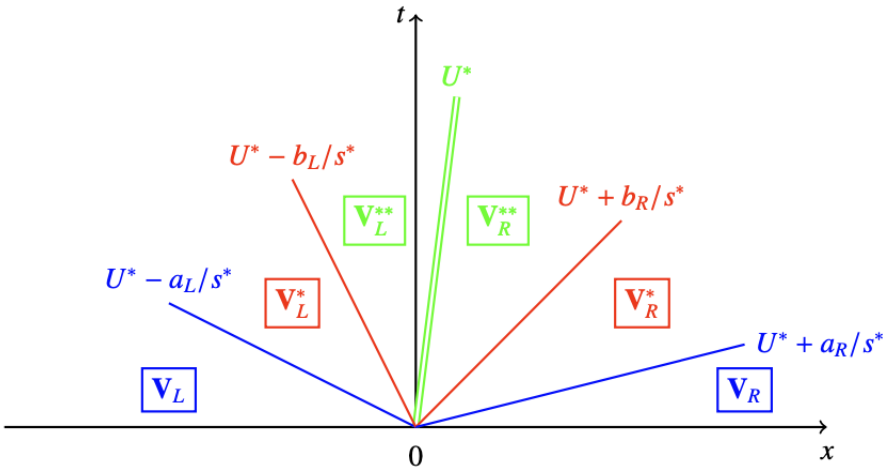

Figure 2: Solution of the Riemann problem for model (3.3)

- *If* $(s_L, s_R) \neq (0,0)$*, i.e., if there is at least a non-empty state, then the quantities defined in* (3.46) *are all well-defined and the solution is non-ambiguous, albeit possibly unphysical (at this stage, we are not yet guaranteed that* s^* *and* $(sc)^*$ *are finite and non-negative).*
- *If* $(s_L, s_R) = (0,0)$*, i.e., if both left and right states are empty, then* c^* *and* U^* *are ill-defined, but if* $\alpha_L + \alpha_R > |U_R - U_L|$ *and if the two states are at equilibrium*[3]*, we have*

$$s^* = 0, \qquad (sc)^* = 0, \qquad (sU)^* = 0, \qquad (scU)^* = 0, \qquad Q^* = 0, \tag{3.47}$$

in an unambiguous way.

Proof. Let us first establish (3.45)-(3.46) before scrutinizing well-definedness. The structure (3.45a) comes from the assumed ordering of waves (3.37). In the components of the intermediate states (3.45b), some Riemann invariants in Proposition (3.1) have been accounted for, such as (a, b, c, Q) across $U \pm a/s$, (a, b, s, U) across $U \pm b/s$, (s, c) across U. Let us write down the remaining Riemann invariants. Across $U \pm a/s$, we have

$$U_L - \frac{a_L}{s_L} = U^* - \frac{a_L}{s^*}, \qquad U^* + \frac{a_R}{s^*} = U_R + \frac{a_R}{s_R}. \tag{3.48}$$

Solving for $(1/s^*, U^*)$, we obtain

$$\frac{1}{s^*} = \frac{a_L/s_L + a_R/s_R}{a_L + a_R} + \frac{U_R - U_L}{a_L + a_R}, \tag{3.49a}$$

[3] a state $\mathbf{V} = (s, c, U, Q, a, b)^T$ is said to be at equilibrium if $U = u(s, c)$ and $Q = q(s, c)$.

$$U^* = \frac{a_R U_L + a_L U_R}{a_L + a_R} + \frac{a_L a_R}{a_L + a_R}\left(\frac{1}{s_R} - \frac{1}{s_L}\right). \tag{3.49b}$$

Across $U \pm b/s$, we have

$$Q_L + b_L c_L = Q^* + b_L c^*, \qquad Q^* - b_R c^* = Q_R - b_R c_R. \tag{3.50}$$

Solving for (c^*, Q^*), we obtain

$$c^* = \frac{b_L c_L + b_R c_R}{b_L + b_R} - \frac{Q_R - Q_L}{b_L + b_R}, \tag{3.51a}$$

$$Q^* = \frac{b_R Q_L + b_L Q_R}{b_L + b_R} - \frac{b_L b_R (c_R - c_L)}{b_L + b_R}. \tag{3.51b}$$

Using $\alpha_L = a_L/s_L$ and $\alpha_R = a_R/s_R$, it is not difficult to verify that (3.49), (3.51) can be rewriten into (3.46). Obviously, these formulas make sense if the denominators do not vanish, which occurs when at least one of the two non-negative saturations s_L and s_R is positive. For the moment, without any further hypothesis, $1/s^*$ may be non-positive and c^* may be negative.

If $\alpha_L + \alpha_R > |U_R - U_L|$, then $\alpha_L + \alpha_R + (U_R - U_L) > 0$ and the limit of

$$s^* = \frac{\alpha_L s_L + \alpha_R s_R}{\alpha_L + \alpha_R + (U_R - U_L)} \tag{3.52}$$

when $s_L, s_R \downarrow 0$ is clearly equal to

$$s^* = 0. \tag{3.53}$$

The limit of U^*, defined in (3.46c) and rewritten as

$$U^* = \frac{\alpha_R (s_R/s_L) U_L + \alpha_L U_R - \alpha_L \alpha_R (s_R/s_L - 1)}{\alpha_L + \alpha_R (s_R/s_L)},$$

is ambiguous, insofar as it depends on the ratio s_R/s_L when $s_L, s_R \downarrow 0$. However, the product

$$s^* U^* = \frac{\alpha_L s_L (U_R + \alpha_R) + \alpha_R s_R (U_L - \alpha_L)}{\alpha_L + \alpha_R + (U_R - U_L)}$$

plainly has an unambiguous limit when $s_L, s_R \downarrow 0$, which is

$$(sU)^* = 0 \tag{3.54}$$

under the condition $\alpha_L + \alpha_R > |U_R - U_L|$. The limit of c^*, defined in (3.46b) and rewritten as

$$c^* = \frac{\beta_L c_L + \beta_R (s_R/s_L) c_R - ((s_R/s_L) Q_R/s_R - Q_L/s_L)}{\beta_L + \beta_R (s_R/s_L)}, \tag{3.55}$$

is ambiguous, insofar as it depends on the ratio s_R/s_L when $s_L, s_R \downarrow 0$. Note that if the left and right states are at equilibrium, the ratios

$$Q_L/s_L = (\gamma_L - 1) c_L u_L, \qquad Q_R/s_R = (\gamma_R - 1) c_R u_R, \tag{3.56}$$

have finite limits when respectively $s_L \downarrow 0$ and $s_R \downarrow 0$. This shows that c^* remains bounded, even though it does not have a limit when $s_L, s_R \downarrow 0$. Therefore, its products with the vanishing s^* and s^*U^* must tend to 0. In other words, we unambiguously have

$$(sc)^* = 0, \qquad (scU)^* = 0. \tag{3.57}$$

Finally, plugging (3.56) into definition (3.46d) of Q^* yields

$$\begin{aligned} Q^* &= s_L s_R \frac{\beta_R(\gamma_L - 1)c_L u_L + \beta_L(\gamma_R - 1)c_R u_R - \beta_L\beta_R(c_R - c_L)}{\beta_L s_L + \beta_R s_R} \\ &= s_R \frac{\beta_R(\gamma_L - 1)c_L u_L + \beta_L(\gamma_R - 1)c_R u_R - \beta_L\beta_R(c_R - c_L)}{\beta_L + \beta_R(s_R/s_L)}, \end{aligned}$$

which admits the unambiguous limit

$$Q^* = 0 \tag{3.58}$$

when $s_L, s_R \downarrow 0$ (as the product of a vanishing s_R and a bounded factor). □

3.5. Conditions on (a, b) to control positivity

Condition $\alpha_L + \alpha_R > |U_R - U_L|$ for the well-definedness of the quantities (3.47) in the Riemann problem when $s_L = s_R = 0$ means that the α_L, α_R must be large enough. It also entails $s_* > 0$ when $(s_L, s_R) \neq (0, 0)$, as shown the upcoming statement.

Lemma 3.3. *Assume that $(s_L, s_R) \neq (0, 0)$ in the Riemann problem. If*

$$\alpha_L + \alpha_R > |U_R - U_L|, \tag{3.59}$$

then the intermediate saturation s^* defined in (3.46a) *is positive. If*

$$(sc)_L\beta_L + (sc)_R\beta_R \geq |Q_R - Q_L|, \tag{3.60}$$

then the intermediate concentration c^* defined in (3.46b) *is non-negative.*

Proof. The two claims are obvious from (3.46a)-(3.46b). □

The drawback of the edge-wise conditions (3.59)-(3.60) is that they couple the coefficients (α, β) of two neighboring cells, unlike the cell-wise conditions (3.28), (3.39). This is why we advocate the slightly stronger but handier cell-wise versions

$$\alpha_L > \tfrac{1}{2}|U_R - U_L|, \qquad \alpha_R > \tfrac{1}{2}|U_R - U_L|, \tag{3.61a}$$

$$\beta_L \geq (\gamma_L - 1)|u_L|, \qquad \beta_R \geq (\gamma_R - 1)|u_R|. \tag{3.61b}$$

The last conditions (3.61b) rely on the assumption that the left and right states are at equilibrium, so that $Q_L = (\gamma_L - 1)s_L c_L u_L$ and $Q_R = (\gamma_R - 1)s_R c_R u_R$. In such a case, division by $(sc)_L$ and $(sc)_R$ does not cause any blow-up when $(sc)_L, (sc)_R \downarrow 0$.

3.6. Update formulas

The space domain is divided into cells $(x_{i-1/2}, x_{i+1/2})$ of uniform size $\Delta x = |x_{i+1/2} - x_{i-1/2}|$. We want to compute an approximation of the average

$$\mathbf{w}_i^n \approx \frac{1}{\Delta x} \int_{x_{i-1/2}}^{x_{i+1/2}} \mathbf{w}(x, t^n)\, \mathrm{d}x$$

for all cell indices $i \in \mathbb{Z}$ and at all time indices $n \in \mathbb{N}$. Each time-step from n to $n+1$ consists of two stages.

3.6.1. Stage 1: Projection on equilibrium manifold ($\varepsilon = 0$)

Having at our disposal $\mathbf{w}_i^n = (s_i^n, s_i^n c_i^n)$ for $i \in \mathbb{Z}$ with $s_i^n \geq 0$, $c_i^n \geq 0$, we first compute the extended states

$$\mathbf{V}_i^n = (s_i^n,\, c_i^n,\, U_i^n,\, Q_i^n,\, a_i^n,\, b_i^n)$$

in which the relaxation variables are forcibly set to equilibrium, that is,

$$U_i^n := u(s_i^n, c_i^n), \qquad Q_i^n := q(s_i^n, c_i^n), \tag{3.62}$$

Formally, formulas (3.62) correspond to $\varepsilon = 0$. Indeed, multiplying (3.3c)-(3.3d) by ε and letting $\varepsilon \downarrow 0$, we obtain

$$0 = s(u(s,c) - U), \qquad 0 = s(q(s,c) - Q). \tag{3.63}$$

The relaxation coefficients are forcibly set as

$$a_i^n = \alpha_i^n s_i^n, \qquad b_i^n = \beta_i^n s_i^n, \tag{3.64}$$

where (α_i^n, β_i^n) is the outcome of the following procedure:

1. Apply (3.28) to compute the Whitham-compliant values

$$\widetilde{\alpha}_i^n = \left\{\mathtt{A}_* + (s u_s)^2 + u_c q_s\right\}^{1/2}(s_i^n, c_i^n), \qquad \widetilde{\beta}_i^n = \left\{\mathtt{B}_* + q_s u_c + (q_c/s)^2\right\}^{1/2}(s_i^n, c_i^n). \tag{3.65a}$$

2. Apply (3.61b) to increase β to the positivity-preserving value

$$\beta_i^n = \max\left\{\widetilde{\beta}_i^n,\ (\gamma_i^n - 1)|u_i^n|\right\}. \tag{3.65b}$$

3. Apply (3.39) to increase α to the Whitham-compliant value

$$\widehat{\alpha}_i^n = \left\{(\widetilde{\alpha}_i^n)^2 + (\beta_i^n)^2 - (\widetilde{\beta}_i^n)^2\right\}^{1/2}. \tag{3.65c}$$

4. Apply (3.61a) to further increase α to the positivity-preserving value

$$\alpha_i^n = \max\left\{\widehat{\alpha}_i^n,\ \tfrac{1}{2}|u_i^n - u_{i-1}^n|,\ \tfrac{1}{2}|u_{i+1}^n - u_i^n|\right\}. \tag{3.65d}$$

3.6.2. Stage 2: Free evolution ($\varepsilon = +\infty$)

Using the piecewise-constant values $\mathbf{V}_i^n$ resulting from stage 1, we next solve the homogeneous part of the relaxation model (3.3). Formally, this stage corresponds to $\varepsilon = +\infty$ and does not "see" the functions $u(s,c)$ and $q(s,c)$. At each edge $i+1/2$, we consider the Riemann problem with left state $\mathbf{V}_L = \mathbf{V}_i^n$ and right state $\mathbf{V}_R = \mathbf{V}_{i+1}^n$. From the solution provided in Theorem 3.3, we extract the quantities sU and $scU+Q$ at the interface (the equation of which is $x/t = 0$ in the local reduced variable x/t). Let us designate by

$$\mathbf{f}_{i+1/2}^{n,\mathrm{Rel}} = \begin{bmatrix} sU \\ scU + Q \end{bmatrix}_{\mathrm{Riem}} (x/t = 0;\, \mathbf{V}_i^n,\, \mathbf{V}_{i+1}^n) \tag{3.66}$$

the value extracted from this operation. Then, the variables of interest are updated by

$$\mathbf{w}_i^{n+1} = \mathbf{w}_i^n - \frac{\Delta t}{\Delta x} \left(\mathbf{f}_{i+1/2}^{n,\mathrm{Rel}} - \mathbf{f}_{i-1/2}^{n,\mathrm{Rel}} \right), \tag{3.67}$$

where $\Delta t = t^{n+1} - t^n > 0$ is the time-step. Note that it is not necessary to update the other conservative variables of the relaxation model such as sU/a^2, sQ/b^2, sa and sb, since the quantities U, Q, a, b will be anyway erased and replaced by those of stage 1 in the next time iteration.

It is also capital to mention that the flux components in (3.66) are always unambiguously defined, even when $s_i^n = s_{i+1}^n = 0$. Indeed, in the latter case:

- If $U_L - \alpha_L > 0$, then the flux components are $s_L U_L = 0$ and $s_L c_L U_L + Q_L = 0$. Likewise, if $U_R + \alpha_R < 0$, the flux components are $s_R u_R = 0$ and $s_R c_R u_R + Q_R = 0$.
- If $U_L - \alpha_L < 0$ and $U_R + \alpha_R > 0$, the four states $\mathbf{V}_L^*$, $\mathbf{V}_L^{**}$, $\mathbf{V}_R^{**}$, $\mathbf{V}_R^*$ that could possibly appear at $x/t = 0$ all have the same saturation s^* and velocity U^*. Hence, the first flux component is $(sU)^* = 0$ by (3.47). The possible concentration values at $x/t = 0$ are c_L, c^* or c_R. Since these numbers are all bounded (despite the fact that c^* is ambiguous), their products with $(sU)^*$ necessarily vanish. On the other hand, $Q_L = Q_R = Q_* = 0$. Thus, the second flux component $scU + Q$ is equal to 0.

Due to the explicit nature of (3.67), the time-step Δt must be subject to a CFL condition which, in combination with the choices (3.65), ensures stability and positivity for the scheme.

Proposition 3.2. *Assume $0 \leq (s)_i^n \leq 1$ and $(sc)_i^n \geq 0$ for all $i \in \mathbb{Z}$. If the relaxation coefficients are chosen in agreement with* (3.65) *and if the time-step is subject to*

$$\frac{\Delta t}{\Delta x} \max_{i \in \mathbb{Z}} \left\{ |u_i^n - \alpha_i^n|,\ |u_i^n + \alpha_i^n| \right\} < \frac{1}{2}, \tag{3.68}$$

then the relaxation scheme (3.67) *satisfies*

$$(s)_i^{n+1} \geq 0, \qquad (sc)_i^{n+1} \geq 0. \tag{3.69}$$

Moreover, by imposing large enough relaxation coefficients, we have $(s)_i^{n+1} \leq 1$.

Proof. Under the CFL condition (3.68) is met, the waves involved in the Riemann problems of any two consecutive edges do not touch each other. The solution $\mathbf{V}^{n+1,-}$ at time $t^{n+1} = t^n + \Delta t$ and just before Godunov's averaging is a piecewise-constant function of x consisting of the intermediate states that appear in each Riemann problem. According to the general theory of Godunov's scheme, it is known [30, 20] that the updated value $\mathbf{w}_i^{n+1} = ((s)_i^{n+1}, (sc)_i^{n+1})$ coming from (3.67) can also be thought of as the averages

$$(s)_i^{n+1} = \frac{1}{\Delta x}\int_{x_{i-1/2}}^{x_{i+1/2}} s(x, t^{n+1,-})\,\mathrm{d}t, \qquad (sc)_i^{n+1} = \frac{1}{\Delta x}\int_{x_{i-1/2}}^{x_{i+1/2}} sc(x, t^{n+1,-})\,\mathrm{d}t. \tag{3.70}$$

If the relaxation coefficients are in agreement with (3.65), then all intermediate states at $(n+1,-)$ have non-negative s and sc. From this and (3.70), the non-negative property (3.69) can be deduced. Similarly, concerning the establishment of the maximum principle to by satisfied by $(s)_i^{n+1}$; namely $(s)_i^{n+1} \leq 1$, according to (3.70) we have to prove that the saturation in the intermediate state at $(n+1,-)$ is smaller than one. Because of (3.49a), the saturation in the intermediate state reads at each interface

$$\frac{1}{s^*_{i+1/2}} = \left(\frac{\alpha_i^n}{\alpha_i^n + \alpha_{i+1}^n}\frac{1}{s_i^n} + \frac{\alpha_{i+1}^n}{\alpha_i^n + \alpha_{i+1}^n}\frac{1}{s_{i+1}^n}\right) + \frac{1}{\alpha_i^n + \alpha_{i+1}^n}\left(u(s_{i+1}^n, c_{i+1}^n) - u(s_i^n, c_i^n)\right). \tag{3.71}$$

Since $s_i^n \leq 1$ for all i in $\mathbb{Z}$, we have to distinguish the case $s_i^n = s_{i+1}^n = 1$ than the others. If $s_i^n = s_{i+1}^n = 1$ then $u(s_i^n, c_i^n) = u(s_{i+1}^n, c_{i+1}^n) = 1$ so that $s^*_{i+1/2} = 1$ and the expected maximum principle is obtained.

Next, assume $s_i^n < 1$ or $s_{i+1}^n < 1$. Since $\alpha_i^n > 0$ and $\alpha_{i+1}^n > 0$ then, arguing a convex combination, we get

$$\frac{\alpha_i^n}{\alpha_i^n + \alpha_{i+1}^n}\frac{1}{s_i^n} + \frac{\alpha_{i+1}^n}{\alpha_i^n + \alpha_{i+1}^n}\frac{1}{s_{i+1}^n} > 1.$$

As a consequence, involving (3.71), there exist α_i^n and α_{i+1}^n large enough such that $s^*_{i+1/2} \leq 1$ and the proof is completed. □

4. Simulation results

The purpose of this section is to compare our relaxation scheme with the upwind scheme. The latter, which is extensively used by reservoir engineers, reads

$$\mathbf{w}_i^{n+1} = \mathbf{w}_i^n - \frac{\Delta t}{\Delta x}\left(\mathbf{f}(\mathbf{w}_i^n) - \mathbf{f}(\mathbf{w}_{i-1}^n)\right). \tag{4.1}$$

This update formula assumes that the underlying model is hyperbolic with positive eigenvalues. In practice, it is used for all IPV laws, even when weak hyperbolicity does not hold.

To carry out this comparison, we focus on the simulation of a polymer flooding experiment in a core that initially contains oil/water without polymer. More

specifically, we consider a one-dimensional domain of length $L_x = 1$ where injection is performed at the left boundary by prescribing a Dirichlet condition. At the right boundary, we produce fluid by imposing an homogeneous Neumann condition. This corresponds to a producer well. The initial saturation in the core is

$$(s,\, c)(x, t = 0) = (0.25, 0), \qquad \forall x \in (0, 1).$$

We inject either pure water or a polymer solution (i.e., a mixture of water and polymer). This setup can be thought of as a highly simplified oil extraction from a reservoir. It is designed in such a way that significant physical information such as the front propagation speeds and the nature of these fronts (rarefaction, shock or contact), which roughly characterize the efficiency of the polymer flooding process, are preserved.

This experiment is performed for two injection scenarios: the continuous injection of a polymer solution (see §4.1) and the injection of a polymer slug (see §4.2). The second scenario amounts to injecting first pure water, next a polymer solution (the polymer slug), then pure water again. In fact, reservoir engineers always have to consider polymer slug injections instead of continuous injection. Their main motivation is to optimize polymer cost and efficiency for oil recovery. Also, they generally have to deal with mature oil reservoirs which have been depleted naturally and/or by water injection during years. To mimic their problem, we consider sequential injections of pure water during a time interval of 0.1 then a polymer solution during a time interval of 0.2 and then pure water. The injections are performed with a constant flow rate and a constant polymer concentration $c_0 = 10^{-4}$.

Regarding physical parameters, we run each scenario with the different IPV models detailed previously: the constant IPV law of §2.2.2 with $\gamma \equiv 1.5$, the percolation law of §2.2.3 with $s_\bullet = 0.1$. For the synthetic law of §2.2.4, the parameters $(s_\bullet,\, \eta)$ have to be appropriately tuned to ensure hyperbolicity for the physical model (2.1). To this end, we set $(s_\bullet,\, \eta) = (0.375,\, 0.01)$. To account for the polymer mobility reduction on water phase, we use formula (2.7) with

$$a_1 = 2 \cdot 10^3, \quad a_2 = 2.8 \cdot 10^5, \quad a_{15/4} = 2.84605 \cdot 10^9.$$

For the petrophysical parameters, we consider the following values:

- for oil phase, the maximal mobility is $\Lambda_o^{\max} = 1$, the Corey exponent m_o is equal to 2 and the residual oil saturation is zero;
- water phase is fixed by maximal mobility is chosen $\Lambda_w^{\mathrm{m}} = 1$, $m_w = 2$ as Corey exponent for water and $s_\flat = 0.2$ as irreducible water saturation.

4.1. Continuous injection of a water and polymer solution

Here, we consider a continuous injection of a water and polymer solution: a mixture made up of water and polymer is injected into the domain at a fixed flow rate and with a constant polymer concentration. Due to our physical

simplifications, this case is equivalent to a Riemann problem with the initial data

$$(s,\, c)(x, t=0) = \begin{cases} (1,\, 10^{-4}) & \text{if } x < 0, \\ (0.25,\, 0) & \text{if } x > 0, \end{cases} \tag{4.2}$$

at least far from the right boundary.

Constant IPV. The results are displayed in Figure 3, where water saturation and polymer concentration profiles in the porous medium at time $T = 0.4$ obtained with 200 and 2000 mesh cells are plotted. With the constant IPV law, the physical model (2.1) is not hyperbolic and the initial states of (4.2) are separated by an elliptic region. No analytical solution is available. The numerical solution exhibits a peak in polymer concentration profile. The amplitude and the position of this peak depend on the number of mesh cells. With $\Delta x = 0.005$, the peak is located at $x = 0.62$ and the ratio between the peak magnitude and the initial polymer concentration is 1.6 for the upwind scheme and 1.4 for the relaxation scheme. For a finer mesh (2000 cells), the peaks created by the two schemes have distinct locations. Besides, the upwind scheme's peak magnitude is higher than the relaxation's one.

To summarize the observations, we can say that this peak increases with several parameters such as the value of γ, the number of mesh cells and the pore volume (PV) injected. In Figure 4, we plot the polymer concentration profile at several intermediate times. The two panels reveal the growth in time of the peak amplitude for the upwind and relaxation schemes. As testified by a straightforward numerical study, the growth is exponential in time. Therefore, this instability is most probably due to an elliptical region rather than a weakly hyperbolic δ-shock.

Anyhow, because this instability is intrinsic to the model, there is no point trying to remove it from the computed solutions. While time-growing peaks are in this case accepted by users as a "fact of life," it is in practice convenient to keep the peak amplitudes low so as to delay as much as possible the code crash. This can be achieved by means of the relaxation scheme using larger values of Whitham parameters, at the price of a greater numerical dissipation.

In Figure 5, we notice that the relaxation scheme reduce the peak amplitude and its growth speed. This figure is obtained by storing for the both schemes the maximum value of polymer concentration in the porous medium. Let us notice that the peak observed with the upwind scheme is not growing continuously (because of mesh discretization) but the values are bounded by two exponential curves.

Percolation IPV. To highlight the benefits of hyperbolicty, we perform simulations with percolation law. The petrophysical parameters are those listed in §4. To set the percolation law, we choose $s_\bullet = 0.1$.

Figure 6 shows simulations performed with the relaxation and upwind schemes for the Riemann problem (4.2). With this law, they also give equivalent results. The results are compared with the exact solution built according to [17]. The

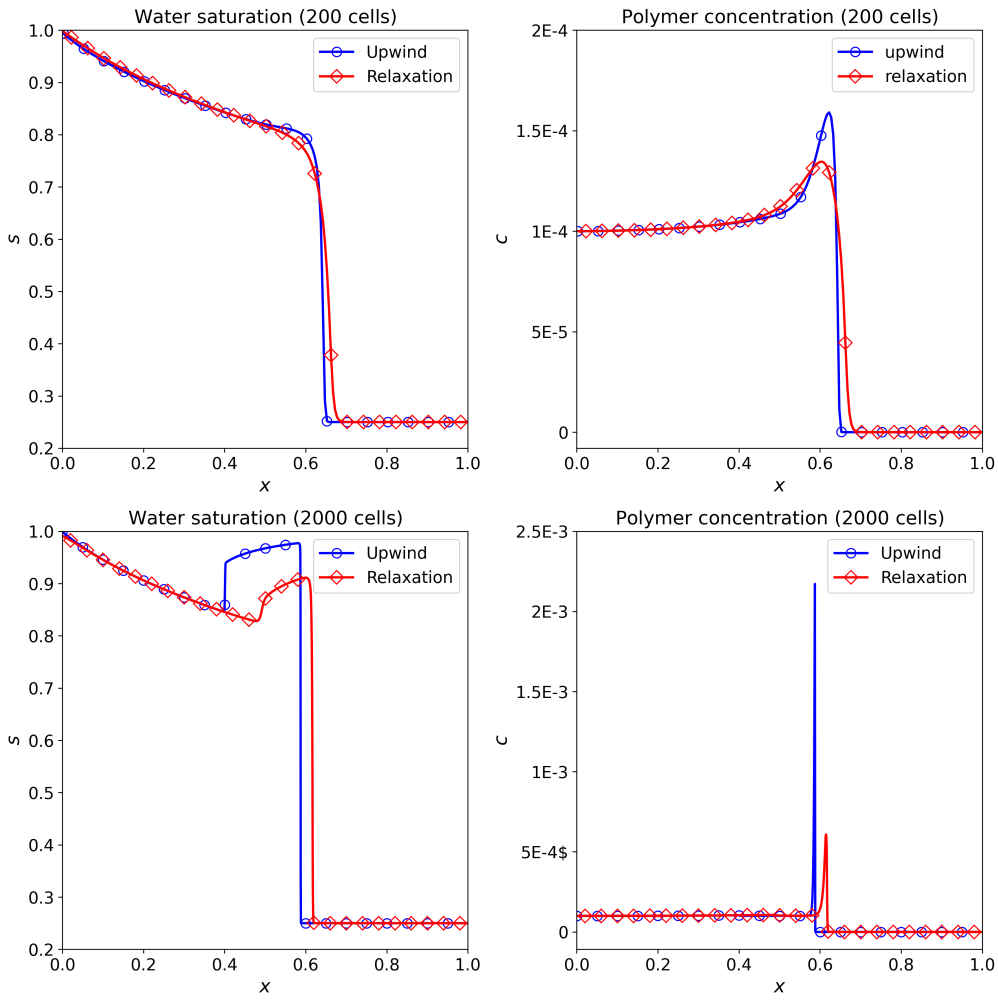

Figure 3: Water saturation (*left*) and polymer concentration (*right*) profiles at time $t = 0.4$ with constant IPV ($\gamma \equiv 1.5$). Results are obtained with 200 (*top*), 2000 (*bottom*) mesh cells and initial data (4.2).

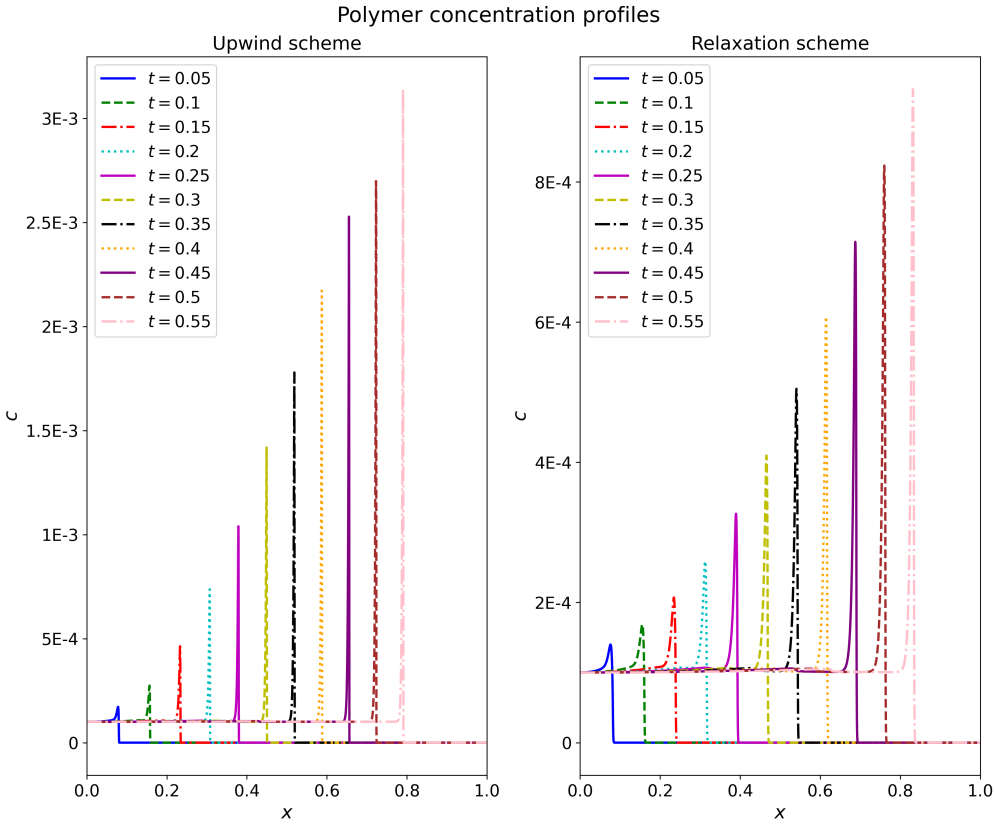

Figure 4: Polymer concentration profiles at different times obtained with upwind (*left*) and relaxation (*right*) schemes with constant IPV ($\gamma \equiv 1.5$) using 2000 mesh cells.

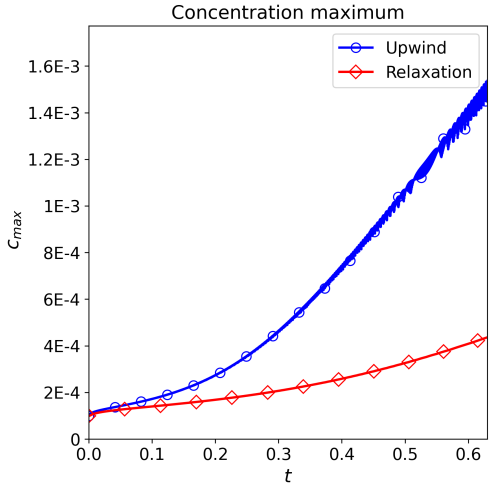

Figure 5: Amplitude of polymer concentration peak versus time with upwind and relaxation schemes. Results are obtained with 1000 mesh cells.

solution structure is the following: for $0 < x < 0.504$ we have a rarefaction wave; at $x = 0.504$, we have the contact discontinuity with the resonance embedded; then, at $x = 0.657$, we have a shock wave. The contact discontinuity is poorly resolved. In fact, at this point we have the resonance and the two waves have the same speed. For more details on schemes convergence, see [18].

We can now assert that with percolation law there is no peak of polymer concentration. The two schemes yield similar results. However, let us recall the condition $s_\bullet < s_\flat$ is not always welcomed by engineers.

Synthetic IPV. We now simulate the Riemann problem (4.2) again, but this time the IPV is chosen to be the synthetic one (2.19).

The results depicted in Figure 7 are obtained with $(s_\bullet, \eta) = (0.375, 0.01)$. Although the relaxation scheme and the upwind scheme provide equivalent results, the relaxation scheme is more time-consuming. By way of example, the upwind scheme with 200 mesh cells takes 2.34 CPU-time (in seconds) while the relaxation scheme takes 20.07 CPU-time. The water saturation profile is similar to that obtained with percolation law. The numerical solution consists of three waves. For $0 < x < 0.45$ we identify a rarefaction. Contrary to percolation law, the polymer concentration seems to remain constant in rarefaction. At $x \simeq 0.45$, we have the first discontinuity. By analogy to the percolation law, we can assume that we have here a contact discontinuity. Finally, we have at $x = 0.667$ a shock which is well represented.

To summarize the observations, we can say that for the weakly hyperbolic model (2.1), the two schemes tend to capture shocks more accurately than contact discontinuities.

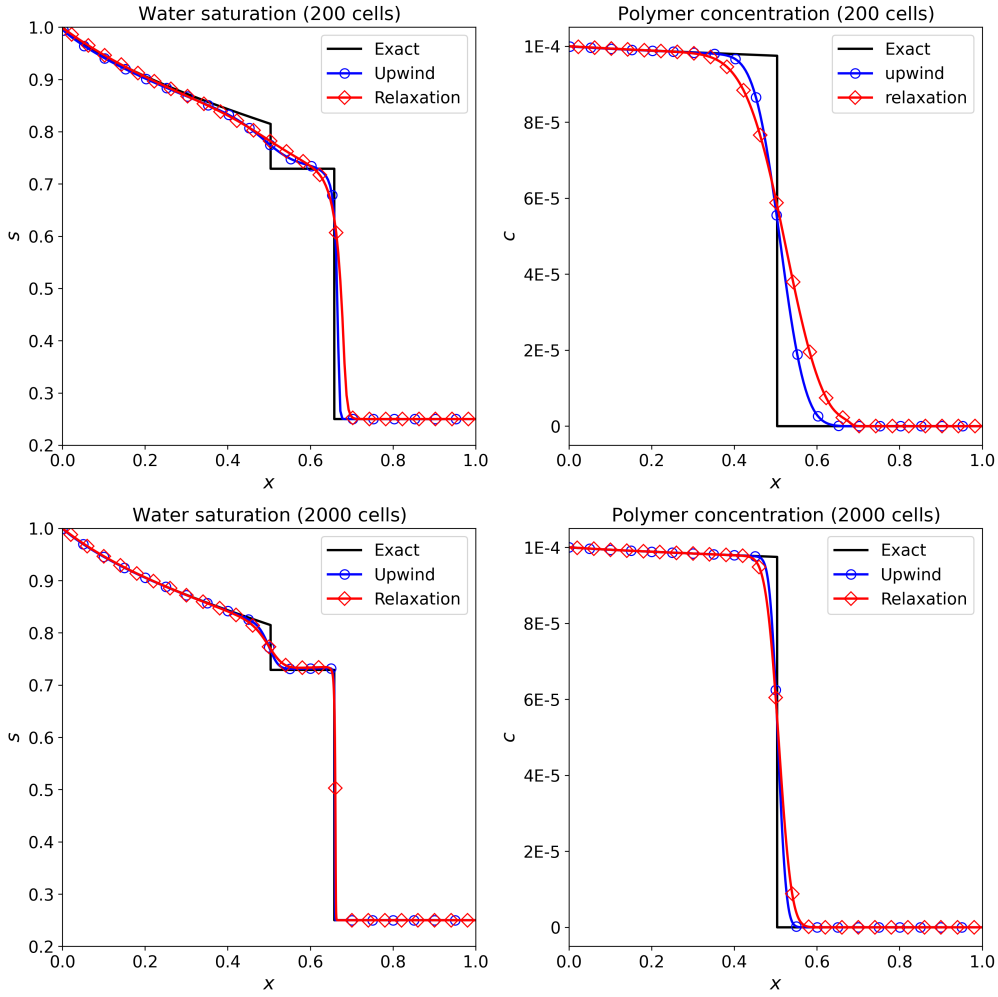

Figure 6: Water saturation (*left*) and polymer concentration (*right*) profiles at time $t = 0.4$ with percolation law ($s_\bullet = 0.1$). Results are obtained with 200 (*top*) and 2000 (*bottom*) mesh cells and initial data (4.2).

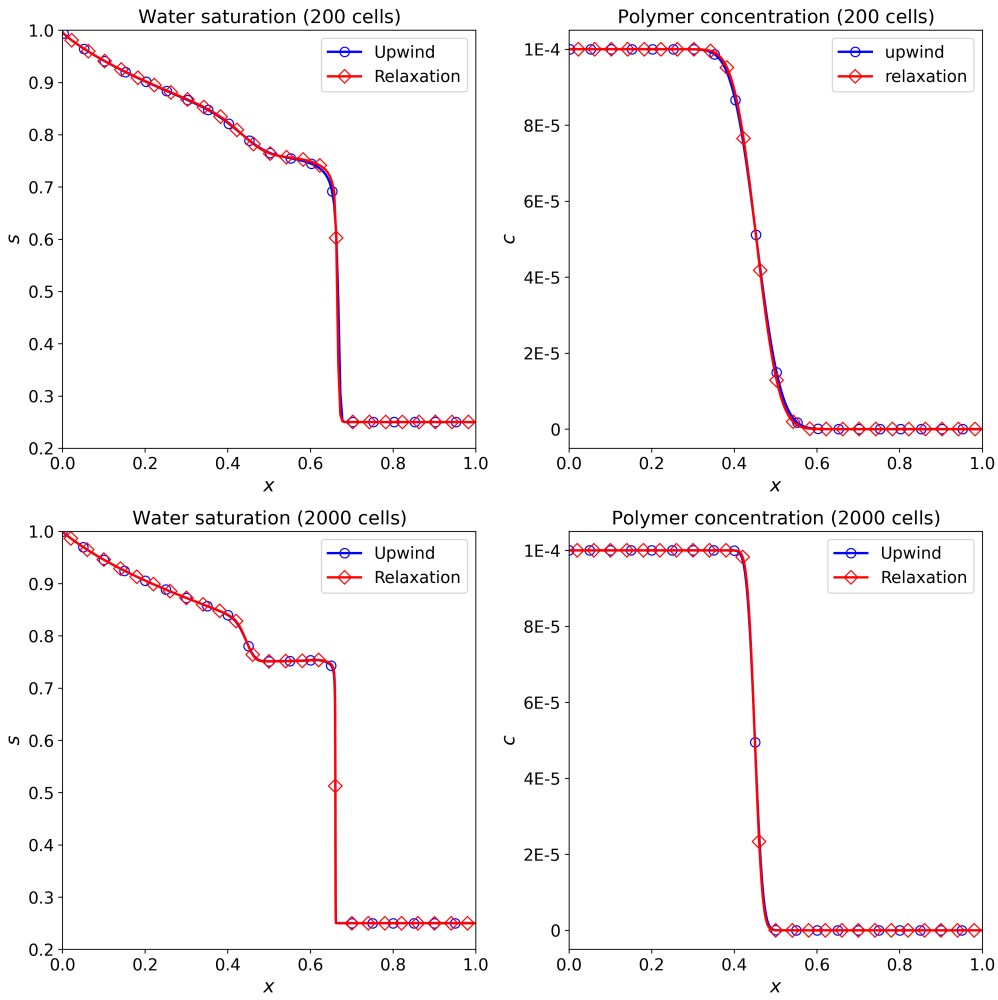

Figure 7: Water saturation (*left*) and polymer concentration (*right*) profiles at time $t = 0.4$ with synthetic IPV law ($s_\bullet = 0.375, \eta = 0.01$). Results are obtained with 200 (*top*) and 2000 (*bottom*) mesh cells and initial data (4.2).

4.2. Polymer slug injection

In this subsection, we consider sequential injections of pure water for $t \in (0, 0.1]$, followed by a polymer solution for $t \in (0.1, 0.3]$, and finally pure water again for $t > 0.3$. The injection is performed at constant flow rate and constant polymer concentration, that is,

$$(s,\, c)(x = 0, t) = \begin{cases} (1,\, 0) & \text{if } \; t \leq 0.1, \\ (1,\, 10^{-4}) & \text{if } \; 0.1 < t \leq 0.3, \\ (1,\, 0) & \text{if } \; t > 0.3. \end{cases} \tag{4.3}$$

Constant IPV. Figure 8 illustrates the water and polymer profiles in the domain at $t = 0.5$, while Figure 9 shows the recordings at producer well. There appears a peak of polymer concentration but we notice that here the water saturation profile is different compared to previous simulations. The front of polymer peak is characterized by an undershoot on water profile and by an overshoot on polymer concentration profile. Regarding the domain output (Figure 9), we have a water breakthrough at about $t = 0.57$. Then, the water flux increases until the polymer peak appears, for $0.57 < t < 0.64$. The water produced corresponds to the *connate* water. During this time slot, the oil production is declining. Then, for $0.64 < t < 0.73$, the polymer starts to exit the domain, pushing the oil better and making the water flux decrease. At $t = 0.73$, there is the polymer peak leading to singularities.

For the upwind scheme, the polymer peak is huge and the water flux reaches the value 1, which indicates that no oil is produced and which is not expected physically. Note that this phenomenon is amplified with a finer mesh. For the relaxation scheme, the polymer peak is negligible in comparison with the one obtained with the upwind scheme. Regarding the water flux, it attains the value 1 only with the finer mesh.

Percolation law. As mentioned earlier, the percolation law has been widely used to simulate this type of problem [2, 23, 9].

In Figure 10, we plot the saturation and polymer concentration profiles obtained with the upwind and the relaxation scheme with 200 and 2000 mesh cells. We clearly see a good agreement between the two numerical scheme. The profiles obtained do not seem singular. With 2000 mesh cells, we see a small amplitude wave at $t = 0.51$ in the water saturation profile. It corresponds to the end of the polymer slug, a contact discontinuity which is not well captured with 200 mesh cell. Also, similarly to the continuous injection case, the polymer concentration is decreasing with water saturation decreasing.

In Figure 11, we plot the water flow rate and the polymer concentration versus time at the producer well. We observe the main tendencies obtained with the constant IPV law whithout the singularities. The connate water is pushed out of the domain. The water breakthrough occurs at $t = 0.59$ and then the water flux increases until $t = 0.82$. Then, the polumer slug exits the domain ($0.82 < t < 1.16$), pushing more oil out and making the water flux slightly decrease. After the polymer slug, the water flux keeps increasing and thus the

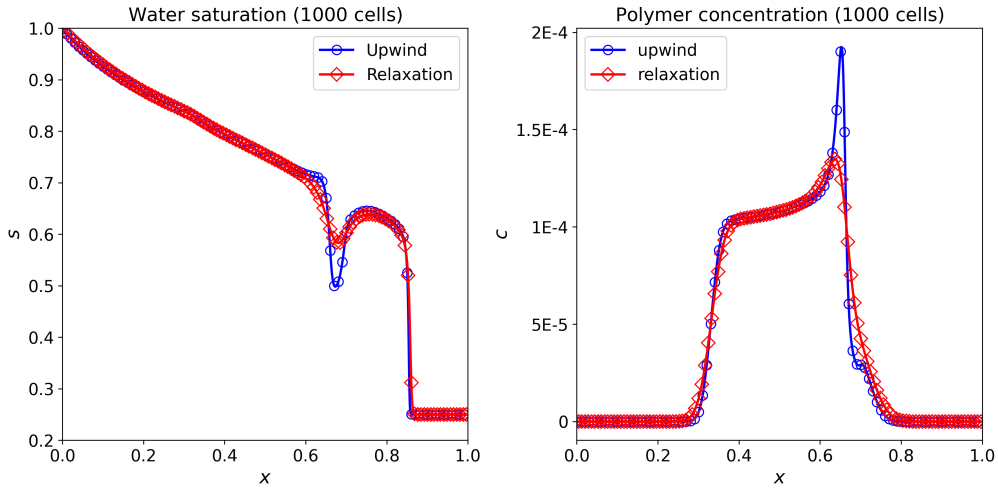

Figure 8: Water saturation (*left*) and polymer concentration (*right*) profiles at time $t = 0.5$ with constant IPV ($\gamma \equiv 1.5$), obtained after pure water / polymer solution / pure water injection. Results are obtained with 1000 mesh cells and initial data (4.2).

oil flux keeps decreasing. Again, we have a very good agreement between the upwind and the relaxation schemes.

Synthetic IPV. In Figure 12, we plot the saturation and polymer concentration profiles obtained with the upwind and the relaxation schemes using 200 and 2000 mesh cells. In Figure 13, we plot the production data for the synthetic IPV.

The results are very close to those obtained with the percolation law. Only the front propagation speed and amplitude have changed. The water breakthrough is obtained at $t = 0.6$ and the polymer slug exists the domain form $t = 0.95$ to $t = 1.25$. As before, no singularity appears and we see that the upwind and relaxation schemes are very close to each other.

5. Conclusion

In this work, we studied a simplified polymer flooding model where the IPV phenomenon was taken into account through various IPV laws. For the three IPV laws considered, the model could be weakly hyperbolic with a resonance curve or contain an elliptic region. Although the traditional upwind scheme was able to cope with all IPV laws, practitioners expressed the need to strengthen robustness in order to go to the end of the simulations involving an unfavorable IPV law, especially those with elliptic instabilities.

We have addressed this need by developing a new numerical scheme based on the relaxation philosophy. This relaxation scheme featured all the benefits that relaxation usually enjoys: (i) it is a dissipative approximation of the original

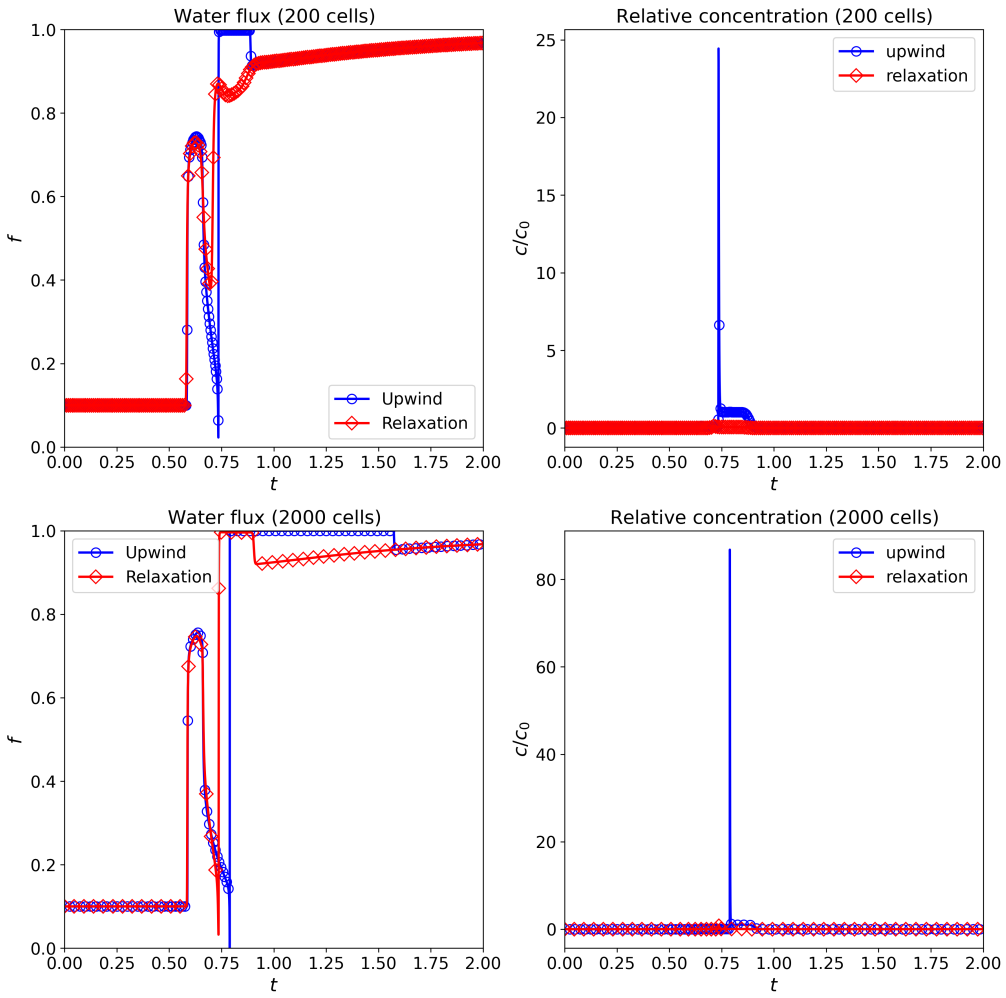

Figure 9: Water flux (*left*) and polymer concentration (*right*) versus time at producer well with constant IPV ($\gamma \equiv 1.5$), obtained after pure water / polymer solution / pure water injection. Results are obtained with 200 (*top*) and 2000 (*bottom*) mesh cells.

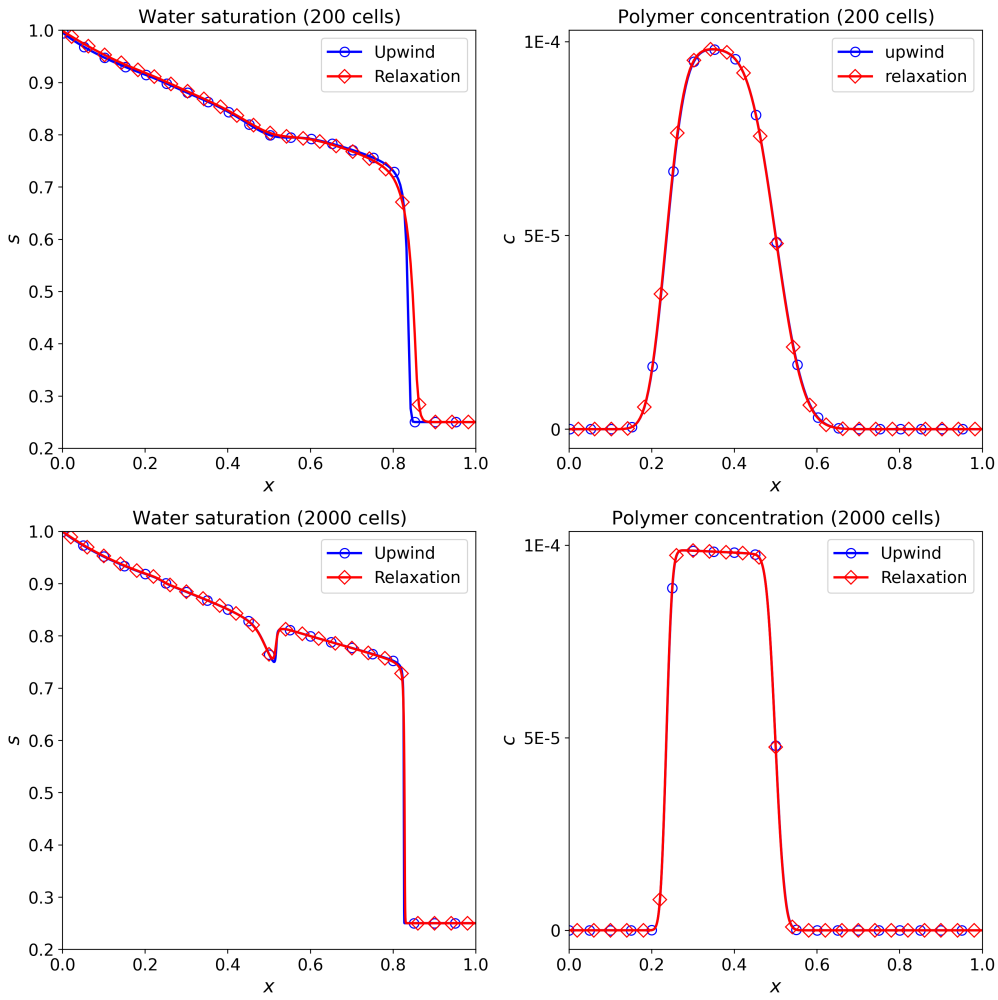

Figure 10: Water saturation (*left*) and polymer concentration (*right*) profiles at time $t = 0.5$ with percolation IPV ($s_\bullet = 0.1$), obtained after pure water / polymer solution / pure water injection. Results are obtained with 200 (*top*) and 2000 (*bottom*) mesh cells.

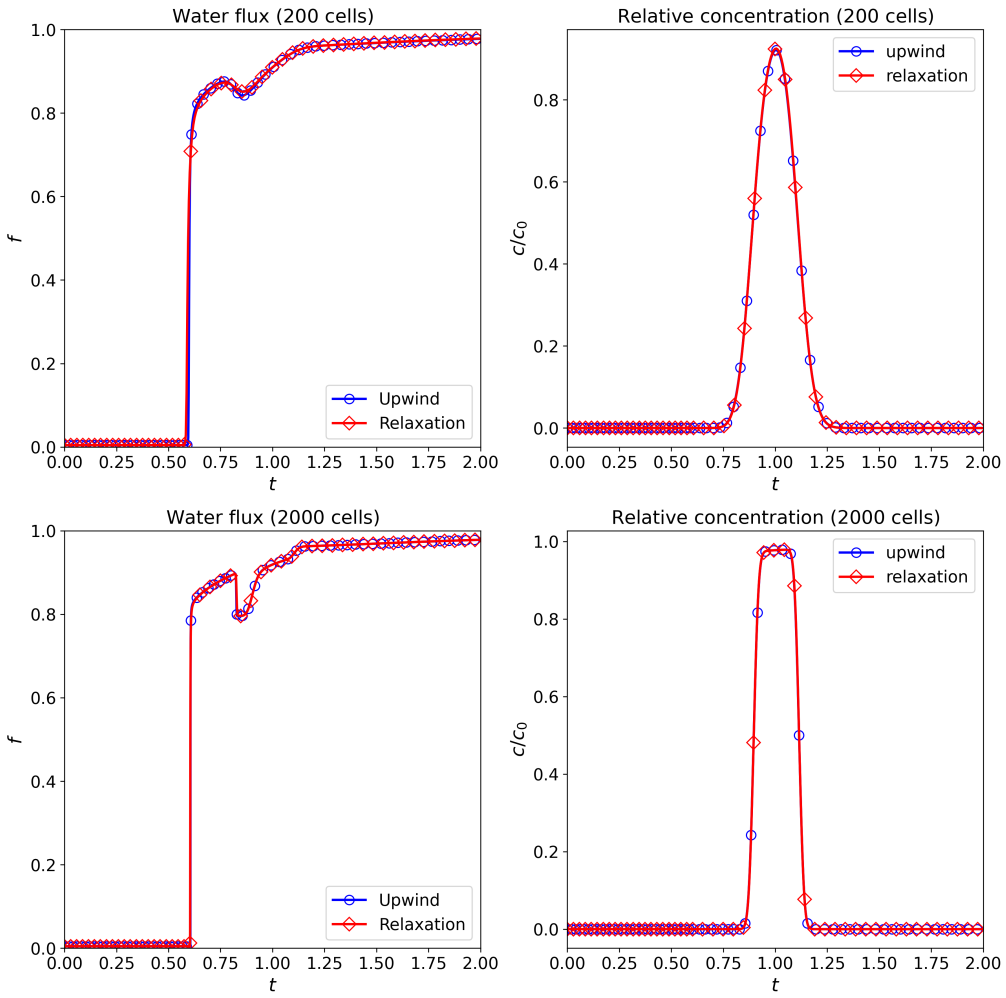

Figure 11: Water flux (left) and polymer concentration (right) versus time at producer well with percolation IPV ($s_\bullet = 0.1$), obtained after pure water / polymer solution / pure water injection. Results are obtained with 200 (*top*) and 2000 (*bottom*) mesh cells.

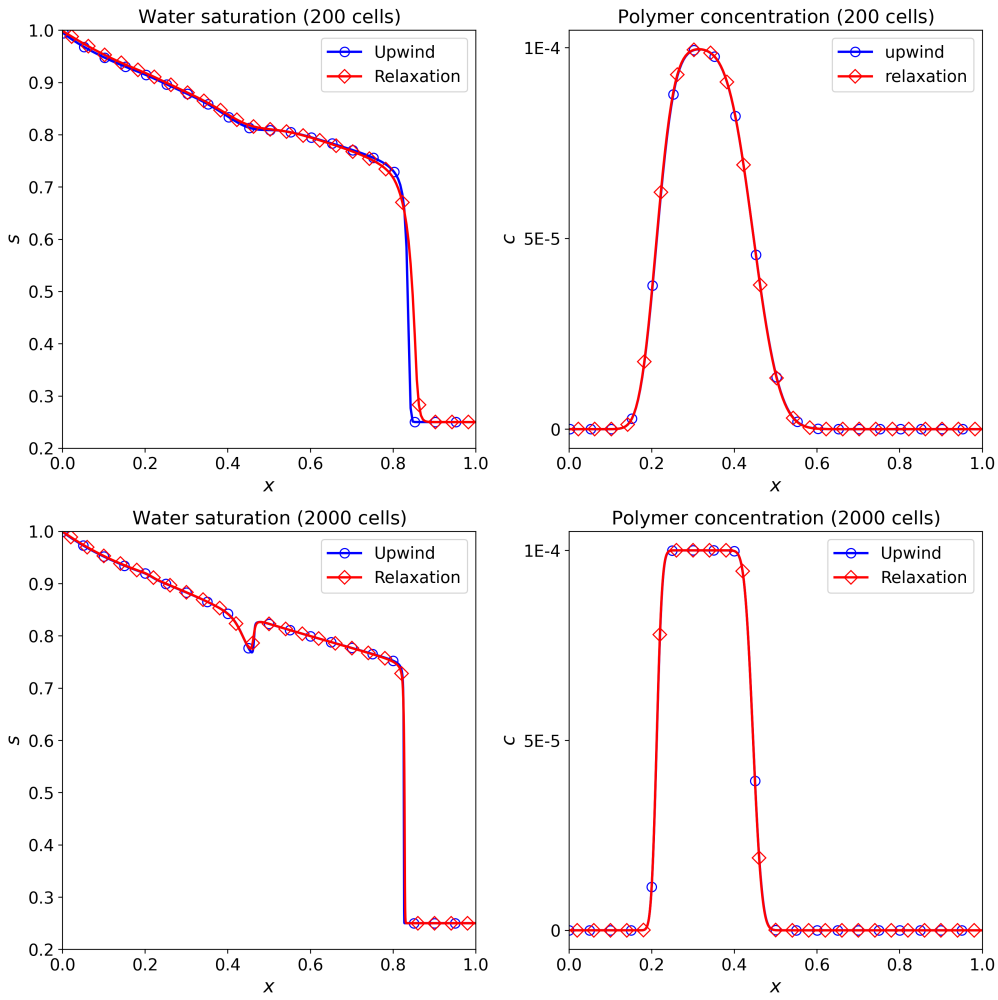

Figure 12: Water saturation (*left*) and polymer concentration (*right*) profiles at time $t = 0.5$ with synthetic IPV ($s_\bullet = 0.375, \eta = 0.01$), obtained after pure water / polymer slug / pure water injection. Results are obtained with 200 (*top*) and 2000 (*bottom*) mesh cells.

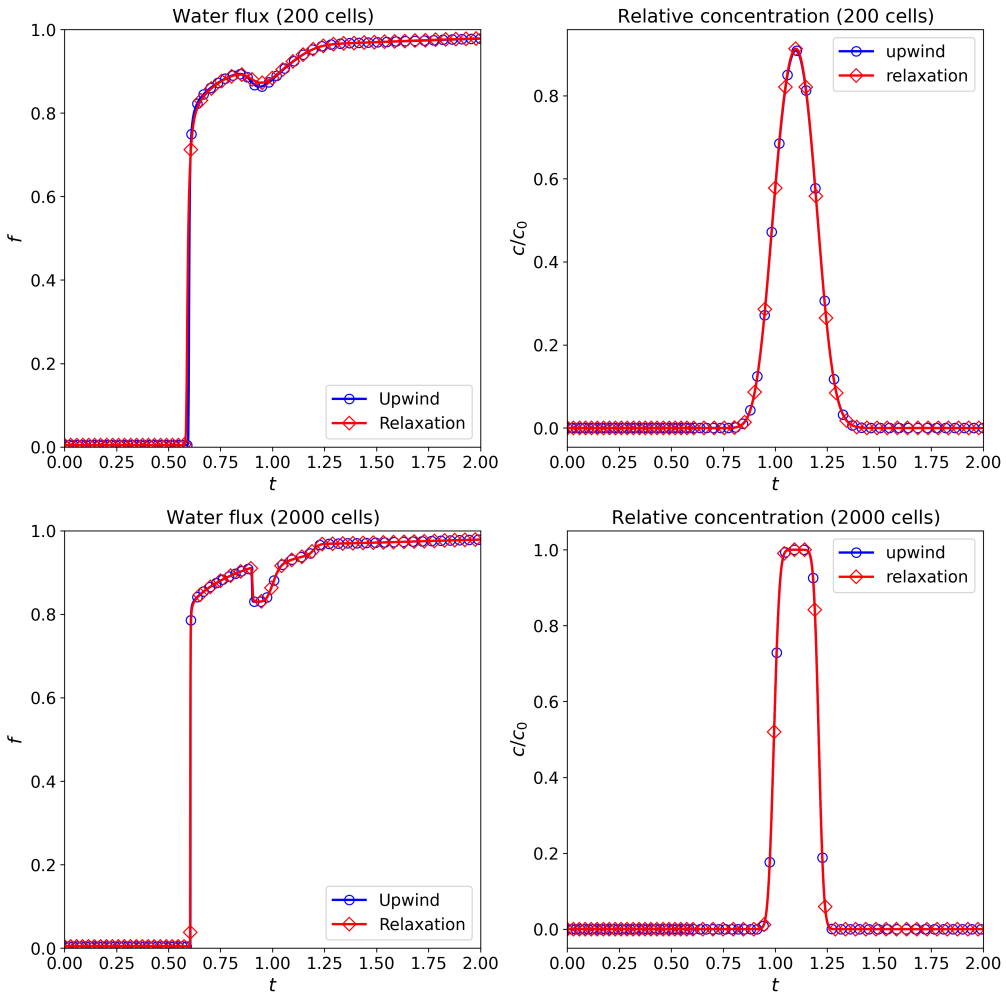

Figure 13: Water flux (*left*) and polymer concentration (*right*) versus time at producer well with synthetic IPV ($s_\bullet = 0.375, \eta = 0.01$), obtained after pure water / polymer solution / pure water injection. Results are obtained with 200 (*top*) and 2000 (*bottom*) mesh cells.

model; (ii) its homogeneous part is unconditionally hyperbolic with all waves linearly degenerated, which makes the Riemann problem very easy to compute; (iii) most importantly, the amount of numerical dissipation can be monitored so as to enforce stability, decrease peak amplitudes and guarantee positivity for s and c.

Numerical results show that upwind scheme and relaxation scheme have equivalent results for favorable IPV laws for which weak hyperbolicity holds everywhere. Even for this kind of laws, the advantage of relaxation scheme is that it appears as more appropriate for those IPV laws that give rise to negative eigenvalues. For unfavorable IPV laws for which there is an elliptic region in the phase space, the differences between the two schemes are slightly more pronounced. In this case, the Whitham parameters of the relaxation scheme enable us to significantly dampen the peak amplitudes in polymer concentration, which in turn lets the simulation run to the end.

Incorporation of the adsorption effect, by which the polymer balance law becomes $\partial_t(sc + a) + \partial_x(fc\gamma) = 0$, where $a \geq 0$ is a non-decreasing function of c, is the obvious next step. As shown in [17, §8.2.2], this can be brought back to the problem without adsorption thanks to a change of variables. In our opinion, more fundamental progress in this area would come from the design of physically more satisfactory synthetic laws, which systematically ensure weak hyperbolicity and of which the contribution [5] is only a first step forward.

Data Availability Statement

The data that support the findings of this study are available from the corresponding author upon reasonable request.

References

[1] E. Audusse, C. Berthon, C. Chalons, O. Delestre, N. Goutal, M. Jodeau, J. Sainte-Marie, J. Giesselmann, and G. Sadaka, *Sediment transport modelling : Relaxation schemes for saint-venant - exner and three layer models*, ESAIM: Proc., 38 (2012), pp. 78–98, https://doi.org/10.1051/proc/201238005.

[2] G. A. Bartelds, J. Bruining, and J. Molenaar, *The modeling of velocity enhancement in polymer flooding*, Transp. Porous Media, 26 (1997), pp. 75–88, https://doi.org/10.1023/A:1006563532277.

[3] M. Baudin, *Méthodes de relaxation pour la simulation des écoulements polyphasiques dans les conduites pétrolières*, PhD thesis, Université Pierre et Marie Curie, 2003, https://hal-ifp.archives-ouvertes.fr/tel-01583001.

[4] M. Baudin, C. Berthon, F. Coquel, R. Masson, and Q. H. Tran, *A relaxation method for two-phase flow models with hydrodynamic closure*

law, Numer. Math., 99 (2005), pp. 411–440, https://doi.org/10.1007/s00211-004-0558-1.

[5] C. Berthon, B. Braconnier, G. L. Dongmo Nguepi, C. Preux, and Q. H. Tran, *Towards weakly hyperbolic models for inaccessible pore volume in polymer flooding*, 2022, https://hal.archives-ouvertes.fr/hal-03627845. submitted.

[6] C. Berthon, M. Breuss, and M.-O. Titeux, *A relaxation scheme for the approximation of the pressureless Euler equations*, Numer. Meth. Part. Diff. Eqs., 22 (2006), pp. 484–505, https://doi.org/10.1002/num.20108.

[7] F. Bouchut, *Nonlinear stability of finite volume methods for hyperbolic conservation laws and well-balanced schemes for sources*, Frontiers in Mathematics, Birkhäuser, Basel, 2004.

[8] B. Braconnier, É. Flauraud, and Q. L. Nguyen, *Efficient scheme for chemical flooding simulation*, Oil Gas Sci. Technol., 69 (2014), pp. 585–601, https://doi.org/10.2516/ogst/2013189.

[9] B. Braconnier, C. Preux, É. Flauraud, Q. H. Tran, and C. Berthon, *An analysis of physical models and numerical schemes for polymer flooding simulations*, Comput. Geosci., 21 (2017), pp. 1267–1279, https://doi.org/10.1007/s10596-017-9637-0.

[10] R. H. Brooks and A. T. Corey, *Hydraulic properties of porous media and their relation to drainage design*, Trans. ASAE, 7 (1964), pp. 26–28, https://doi.org/10.13031/2013.40684.

[11] S. E. Buckley and M. C. Leverett, *Mechanism of fluid displacement in sands*, Trans. AIME, 146 (1942), pp. 107–116, https://doi.org/10.2118/942107-G.

[12] C. Chalons and J.-F. Coulombel, *Relaxation approximation of the Euler equations*, J. Math. Anal. Appl., 348 (2008), pp. 872–893, https://doi.org/10.1016/j.jmaa.2008.07.034.

[13] G.-Q. Chen, C. D. Levermore, and T.-P. Liu, *Hyperbolic conservation laws with stiff relaxation terms and entropy*, Commun. Pure Appl. Math., 47 (1994), pp. 787–830, https://doi.org/10.1002/cpa.3160470602.

[14] F. Coquel and B. Perthame, *Relaxation of energy and approximate Riemann solvers for general pressure laws in fluid dynamics*, SIAM J. Numer. Anal., 35 (1998), pp. 2223–2249, https://doi.org/10.1137/S0036142997318528.

[15] R. Dawson and R. B. Lantz, *Inaccessible pore volume in polymer flooding*, SPE Journal, 12 (1972), pp. 448–452, https://doi.org/10.2118/3522-PA.

[16] P.-G. de Gennes, *Scaling Concepts in Polymer Physics*, Cornell University Press, Ithaca, 1979.

[17] G. L. Dongmo Nguepi, *Modèles mathématiques et numériques avancés pour la simulation du polymère dans les réservoirs pétroliers*, PhD thesis, Université Paris-Saclay, 2021, https://tel.archives-ouvertes.fr/tel-03518783.

[18] G. L. Dongmo Nguepi, B. Braconnier, C. Preux, Q. H. Tran, and C. Berthon, *Glimm and finite volume schemes for polymer flooding model with and without inaccessible pore volume law*, in ECMOR XVII Conference Proceedings, September 14-17, European Association of Geoscientists & Engineers, 2020, pp. 1–21, https://doi.org/10.3997/2214-4609.202035090.

[19] G. L. Dongmo Nguepi, B. Braconnier, C. Preux, Q.-H. Tran, and C. Berthon, *A relaxation method for the simulation of possibly non-hyperbolic polymer flooding models with inaccessible pore volume effect*, in Finite Volumes for Complex Applications IX - Methods, Theoretical Aspects, Examples, R. Klöfkorn, E. Keilegavlen, F. A. Radu, and J. Fuhrmann, eds., Cham, 2020, Springer International Publishing, pp. 445–453, https://doi.org/10.1007/978-3-030-43651-3_41.

[20] E. Godlewski and P.-A. Raviart, *Numerical Approximation of Hyperbolic Systems of Conservation Laws*, vol. 118 of Applied Mathematical Sciences, Springer-Verlag, New York, 1996.

[21] D. W. Green and G. P. Willhite, *Enhanced Oil Recovery*, vol. 6 of SPE Textbook Series, Society of Petroleum Engineers, 1998.

[22] A. Harten, P. D. Lax, and B. van Leer, *On upstream differencing and Godunov-type schemes for hyperbolic conservation laws*, SIAM Rev., 25 (1983), pp. 35–61, https://doi.org/10.1137/1025002.

[23] S. Hilden, H. Nilsen, and X. Raynaud, *Study of the well-posedness of models for the inaccessible pore volume in polymer flooding*, Transp. Porous Media, 114 (2016), pp. 65–86, https://doi.org/10.1007/s11242-016-0725-8.

[24] M. L. Huggins, *Solutions of long chain compounds*, J. Chem. Phys., 9 (1941), p. 440, https://doi.org/10.1063/1.1750930.

[25] E. L. Isaacson and J. B. Temple, *Analysis of a singular hyperbolic system of conservation laws*, J. Diff. Eqs, 65 (1986), pp. 250–268, https://doi.org/10.1016/0022-0396(86)90037-9.

[26] S. Jin and M. Slemrod, *Regularization of the Burnett equations via relaxation*, J. Stat. Phys., 103 (2001), pp. 1009–1033, https://doi.org/10.1023/A:1010365123288.

[27] S. Jin and Z. Xin, *The relaxation schemes for systems of conservation laws in arbitrary space dimensions*, Commun. Pure Appl. Math, 48 (1995), pp. 235–277, https://doi.org/10.1002/cpa.3160480303.

[28] B. L. Keyfitz and H. C. Kranzer, *A system of non-strictly hyperbolic conservation laws arising in elasticity theory*, Arch. Rat. Mech. Anal., 72 (1980), pp. 219–241, https://doi.org/10.1007/BF00281590.

[29] L. W. Lake, *Enhanced Oil Recovery*, Prentice Hall, Englewood Cliffs, New Jersey, 1989.

[30] R. J. LeVeque, *Numerical Methods for Conservation Laws*, Lectures in Mathematics ETH Zürich, Birkhäuser Verlag, Basel, 1992.

[31] J. Liu, M. Delshad, G. A. Pope, and K. Sepehrnoori, *Application of higher-order flux-limited methods in compositional simulation*, Transp. Porous Media, 16 (1994), pp. 1–29, https://doi.org/10.1007/BF01059774.

[32] T. P. Liu, *Hyperbolic conservation laws with relaxation*, Commun. Math. Phys., 108 (1987), pp. 153–175, https://doi.org/10.1007/BF01210707.

[33] A. Majda and R. L. Pego, *Stable viscosity matrices for systems of conservation laws*, J. Diff. Eqs, 56 (1985), pp. 229–262, https://doi.org/10.1016/0022-0396(85)90107-X.

[34] G. A. Pope, *The application of fractional flow theory to enhanced oil recovery*, SPE Journal, 20 (1980), pp. 191–205, https://doi.org/10.2118/7660-PA.

[35] P. L. Roe, *Approximate Riemann solvers, parameter vectors and difference schemes*, J. Comput. Phys., 43 (1981), pp. 357–372, https://doi.org/10.1016/0021-9991(81)90128-5.

[36] N. Saad, G. A. Pope, and K. Sepehrnoori, *Application of higher-order methods in compositional simulation*, SPE Reserv. Engin., 5 (1990), pp. 623–630, https://doi.org/10.2118/18585-PA.

[37] P. Saffman and G. Taylor, *The penetration of a fluid into a porous medium or Hele-Shaw cell containing a more viscous liquid*, Proc. R. Soc. A, 245 (1958), pp. 312–329, https://doi.org/10.1098/rspa.1958.0085.

[38] K. S. Sorbie, *Polymer-Improved Oil Recovery*, Springer Science, New York, 1991, https://doi.org/10.1007/978-94-011-3044-8.

[39] I. Suliciu, *On modelling phase transitions by means of rate-type constitutive equations. shock wave structure*, Int. J. Engin. Sci., 28 (1990), pp. 829–841, https://doi.org/10.1016/0020-7225(90)90028-H.

[40] I. Suliciu, *On the thermodynamics of fluids with relaxation and phase transitions. fluids with relaxation*, Int. J. Engin. Sci., 36 (1998), pp. 921–947, https://doi.org/10.1016/S0020-7225(98)00005-6.

[41] G. B. Whitham, *Linear and nonlinear waves*, Pure and Applied Mathematics, Wiley-Interscience, New York, 1974.